6

LOPINAVIR

AND

MSNs

6. Lopinavir and MSNs

Experimental

6.1 Synthesis procedure for MCM-41NPs, MCM-48NPs and SBA-15NPs

Synthesis procedure for MCM-41NPs, MCM-48NPs and SBA-15NPs is described in section 5.1 A, B and C

6.2 Characterization of Mesoporous MCM-41NPs

Characterizations of synthesized MCM-41NPs, MCM-48NPs and SBA-15NPs is described in section 5.2 A, B and C

Optimization of drug loading procedure

The drug loading process was optimized with respect to drug: carrier ratio.

The ratio of drug as to carrier

An important parameter for maximum drug loading into the mesopores is to select the proper ratio of LPV and carriers (MCM-41NPs, MCM-48NPs and SBA-15NPs). Different ratios were tried and checked for drug loading. Also the effect of different solvents, stirring rate and time effect on drug loading was also checked.

6.3 LPV loading in mesoporous silica nanoparticles (MSNs)

MCM-41NPs, MCM-48Nps and SBA-15NPs were used for drug loading process. Before using these MSNs for drug loading the MSNs were kept in the oven at 80°C for 30 min in to remove the moisture contain from the pores of mesostructure. A solvent evaporation technique was used for drug loading. The MCM-41NPs was placed as the powder into the methanolic solution that contained drug of given concentration. The drug loading procedure is described below.

In preliminary drug loading procedure, LPV (100mg) was dissolved in methanol solvent (10 ml) and then MCM-41NPs (150 mg) was added. The mixture was stirred for 1-2h at room temperature to achieve maximum drug loading and then the methanol was recovered by solvent evaporation method at 50°C on Bucchi rotary evaporator until complete dry powder of MCM-41NPs was obtained. The recovered solid LPV loaded MCM-41NPs were dried at room temperature and store in dry place for further use. After LPV loaded in MCM-41NPs it was designated as L-MCM-41NPs.

The same above procedure was used for the LPV loading in MCM-48NPs and SBA-15NPs. And it was designated as L-MCM-48NPs and L-SBA-15NPs. All LPV loaded mesoporous silica nanoparticles designated as L-MSNs-NPs

6.4 Characterization of LPV loaded Mesoporous silica nanoparticles (L-MSNs-NPs)

The LPV drug loaded different MSNs (MCM-41 NPs, MCM-48NPs and SBA-15NPs) were characterized and evaluated by DSC, FT-IR, powder-XRD, N2-adsorption isotherm in a similar manner which is already described in section 5.2. The entrapment efficiency (EE) and loading efficiency (LE) for the different MSNs was determined by UV spectrophotometric method at 220nm wavelength and thermogravimetric analysis respectively. The same procedure and formula for calculating entrapment efficiency and loading efficiency of LPV and MSNs was used that are mentioned in chapter 5, section 5.4.

6.5 Formulation of L-MSNs and LR-MSNs tablet and evaluation

For In vitro dissolution study drug loaded mesoporous silica nanoparticles were formulated in tablets by direct compression method. L-MCM-48NPs equivalent to 200 mg LPV and different excipients like Low- Hydroxypropyl cellulose (L-HPC), microcrystalline cellulose, cross-povidone, lactose monohydrate (SUPERTAB 11SD) [1] (all excipients was sifted through ASTM 25#) mixed thoroughly for 15 min and then add magnesium stearate (sifted through ASTM 60#) was added. The mixture was blended for 03 min and punched in single rotary tablet machine having 16*9 mm diameter punches with flat faced beveled edges. The same procedure was followed for L-MCM-41NPs and L-SBA-15NPs for preparations of tablets. Lopinavir tablet composition by L-MSNs is given below in table 6.1

Table 6.1 Lopinavir Tablet Formulation Composition

Ingredients	Quantity (mg/tablet)
L-MCM-48NPs*	500
microcrystalline cellulose PH102	120
lactose monohydrate (SUPERTAB 11SD)	65
cross-povidone	30
Low-Hydroxypropyl cellulose (L-HPC)	30
magnesium stearate	5
Total weight	750

*Remarks: For MCM-41 and SBA-15 nanoparticles equivalent to 200 mg Lopinavir were taken and tablet weight was adjusted with Microcrystalline cellulose PH 102.

As commercially available tablet formulation is combination of lopinavir/ritonavir (200/50 mg).[3] Our final target was also to develop combination formulation of lopinavir/ritonavir loaded MSNs. For this ritonavir silica nanoparticles (R-MSNs) were taken as developed earlier in section 5. R-MSNs equivalent to 50mg RTV was physically mixed with L-MSNs-NPs equivalent to 200 mg of LPV. The selected

excipients were then mixed to get final tablet formulation. All material blended and punched in a single rotary tablet machine having 18*9 mm diameter punches with flat faced beveled edges. Prepared tablets were designated as LR-MCM-48NPs, LR-MCM-41NPs and LR-SBA-15NPs. (LR-MSNs). All the excipients used in both tablet preparations are safe as per GRAS.[1] Lopinavir/Ritonavir tablet composition by L/R-MSNs are given below in table 6.2

Table 6.2 Lopinavir + Ritonavir Tablet Formulation Composition

Ingredients	Quantity (mg/tablet)
L-MCM-48NPs*	500
R-MCM-48NPs*	125
microcrystalline cellulose PH102	120
lactose monohydrate (SUPERTAB 11SD)	65
cross-povidone	30
Low-Hydroxypropyl cellulose (L-HPC)	30
magnesium stearate	5
Total weight	900

*Remarks: For MCM-41 and SBA-15 nanoparticles equivalent to 200 mg Lopinavir and 50 mg Ritonavir respectively were taken and tablet weight was adjusted with Microcrystalline cellulose PH 102.

All prepared tablets were evaluated by various parameters such as weight variation, hardness, friability and disintegration time etc.

6.6 *In-vitro* dissolution study

In-vitro dissolution study was performed in dissolution apparatus (Veego dissolution test apparatus). Six dissolution units were studied for In-vitro dissolution of the LPV pure drug and L-MSNs. L-MCM-41NPs, L-MCM-48NPs and L-SBA-15NPs equivalent to 100 mg tablets of LPV, pure drug LPV tablets and MF were taken for the in-vitro dissolution study. In vitro dissolution studies were carried out in the (A) pH 1.2±0.1 hydrochloric acid solution (0.1N HCl) with 0.75% PLE, (B) Acetate buffer pH 4.5 with 0.75% PLE and (C) Phosphate buffer pH 6.8 with 0.75% PLE media using USP dissolution apparatus II with paddle rotating speed 50rpm in 900 mL media volume at 37±0.5°C temperature. At predetermined time intervals of 10, 20, 30, 45 and 60 min, five mL of dissolution sample was removed from the vessels with the help of cannula, replacing the same amount with fresh dissolution medium. Collected samples were filtered through 0.22µm syringe filter and LPV content was determined by using RP-HPLC method.

The same procedure was used for *in-vitro* dissolution study of LR-MSNs to evaluate effect of RTV on in vitro release pattern of LPV. The LPV content was determined by RP-HPLC method.

6.7 *In-vivo* pharmacokinetic study for LPV

In this study, pharmacokinetic behaviours of the prepared L-MSNs, LR-MSNs and pure LPV, combination of LPV/RTV and MF were investigated to determine the oral bioavailability of LPV. The plots of drug plasma concentration Vs time were plotted for LPV after oral administration of L-MSNs, LR-MSNs and compared it with plain LPV, combination of LPV/RTV and MF. Non compartmental pharmacokinetic analysis was performed. Various pharmacokinetic parameters like C_{max}, t_{max}, $t_{1/2}$ and Area Under Curve (AUC) were calculated by using plasma concentration Vs time profile curve using PK solver software and results are shown as mean±SD.

6.7.1 Animals

The protocol was same as described in Section 5.7.1.

6.7.2 Experimental: Dosing and sampling

Relative bioavailability of L-MSNs and LR-MSNs were evaluated by comparing the bioavailability of L-MSNs and LR-MSNs with bioavailability of plain LPV, combination of LPV/RTV and MF. Albino wistar rats were divided in nine groups and each group hold 3 rats. Prior the experiment all wistar rats kept on fasted condition for overnight with free access of water. The bioavailability of L-MCM-41NPs, L-MCM-48NPs and L-SBA-15NPs (L-MSNs) and LR-MCM-41NPs, LR-MCM-48NPs and LR-SBA-15NPs (LR-MSNs) were compared with the pure LPV, combination of pure LPV/RTV and MF. The pure LPV and L-MSNs equivalent to 20 mg/kg dose of LPV and combination of LPV/RTV and LR-MSNs equivalent to 20/5 mg/kg dose of LPV/RTV were dispersed in 2 mL of CMC solution (0.5% w/v) and administrated orally to wistar rat. Approx. 0.3ml blood samples were collected through the retro-orbital vein into 60 µL EDTA (0.5%w/v) containing micro centrifuge tubes at 0, 1, 1.5, 2, 2.5, 4, 6, 8, 12 and 16 h after oral administration. Collected blood samples were mixed with the anticoagulant by properly shaking and centrifuged at 5000 rpm for 10 min at 4ºC using a centrifuge machine and then plasma samples were collected and stored at -20°C.

6.7.3 Instrumental and statistical analysis

Collected plasma samples were extracted and analyzed by using developed RP-HPLC method (Chapter 3, Section 3.2.2.4). The LPV concentrations in plasma were determined by using the calibration curve. Non-compartmental trapezoidal method was used to calculate the area under the curve (AUC) of plasma concentration as a function of time (t). All data were reported as mean ± SD.

6.8 Cell Line Studies of LPV and it's formulations using Caco-2 cell line model

6.8.1.1 In-vitro cytotoxicity study (MTT assay)

Cytotoxicity study of pure LPV and L-MCM-48NPs, L-SBA-15NPs was evaluated by method described in chapter 5, section 5.8.2.1

6.9 Stability study of L-MSNs

Physical and chemical stability of L-MSNs were evaluated same as per procedure mention in chapter 5 section 5.9.2

RESULT AND DISCUSSION

6.10 Synthesis of MCM-41NPs, MCM-48NPs and SBA-15NPs (MSNs)

Synthesis procedure for MCM-41NPs, MCM-48NPs and SBA-15NPs was described in section 5.1

6.11 Characterization of MCM-48NPs, MCM-41NPs and SBA-15NPs (MSNs)

Mesoporous MCM-48NPs, MCM-41NPs and SBA-15NPs MSNs were characterized as described in section 5.2.

6.12 LPV loading in Mesoporous Silica Nanoparticles (MSNs)

For LPV loading in MSNs, the same solvent evaporation method was used. The procedure for solvent evaporation method for drug loading in MSNs was described earlier in chapter 5 section 5.3. The same principle for RTV loading in MSNs is followed by LPV loaded in MSNs and that is same as described in chapter 5 section 5.12.

The probable mechanism of drug loading is that, the a C=O group of amide and oxygen of ether group of LPV would form hydrogen bonds with the silanol groups (Fig 6.1) of developed mesoporous silica nanoparticles and consequently drug molecules would be retained into the mesopores.[2-4]

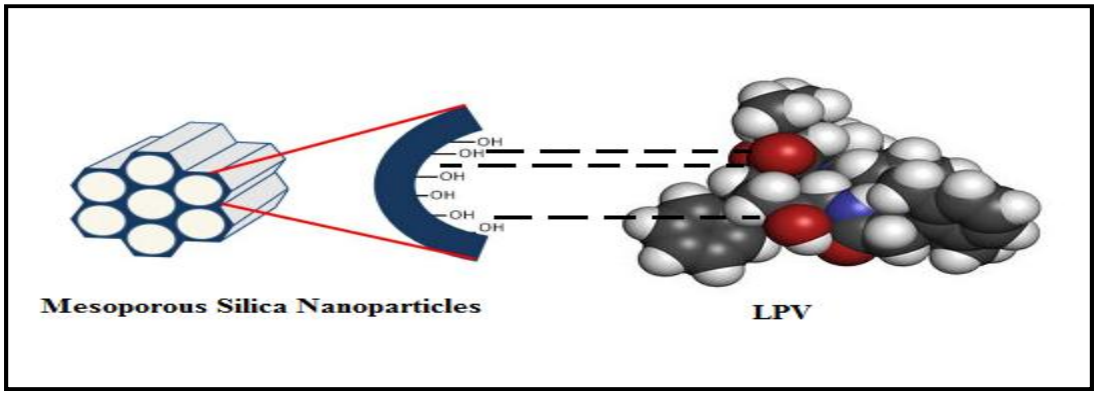

Figure 6.1 Graphical representation of LPV linkage to silanol group of MSNs[5]

6.13 Optimization of drug loading procedure

The drug loading process was optimized by ratio of drug and drug carrier (MSNs).

6.13.1 Ratio of drug to carrier

To achieve maximum drug loading in carriers, optimization of the ratio of drug to carrier is important. For that different proportions of drug to carrier ratio were taken. Four different LPV as to carrier proportions were tested i.e. 1:1, 1:1.25, 1:1.5 and 1:2. In Fig.6.2, 6.3, 6.4 show DSC thermograms of LPV with varied carrier ratio. For

measuring the amount of LPV entrapped in MSNs the same UV spectrophotometric method (described in Chapter 3, Section 3.2) was used.

The % Entrap efficiency of drug and % loading efficiency for MSNs were calculated by using a formula mentioned in chapter 5, section 5.4. The maximum drug loading was achieved with 1:1.5 weight ratio and % entrapment efficiency of LPV in MCM-48NPs was 98.13%, for MCM-41NPs it was 87.34% and for SBA-15NPs it was 99.45%. Factors such as different solvents e.g. acetonitrile, mixture of acetonitrile and methanol and stirring rate and time did not affect the % loading efficiency of LPV in all mesoporous silica nanoparticles. The results of drug loading procedure are shown in table 6.3

Table 6.3 Effects of drug: MSNs ratio on drug loading

Weight ratio Drug: Carrier	% Drug loading in MCM-48NPs	% Drug loading in MCM-41NPs	% Drug loading in SBA-15NPs	DSC result	Remarks
1:1	-	-	-	Sharp fusion peak of LPV was observed	LPV not totally entrapped in all MSNs
1:1.25	-	-	-	Sharp fusion peak of LPV was observed	LPV not totally entrapped in all MSNs
1:1.5	49%	40%	57%	No fusion peak of LPV was observed	LPV was totally entrapped in all MSNs
1:2	45%	37%	51%	No fusion peak of LPV was observed	LPV was totally entrapped in all MSNs

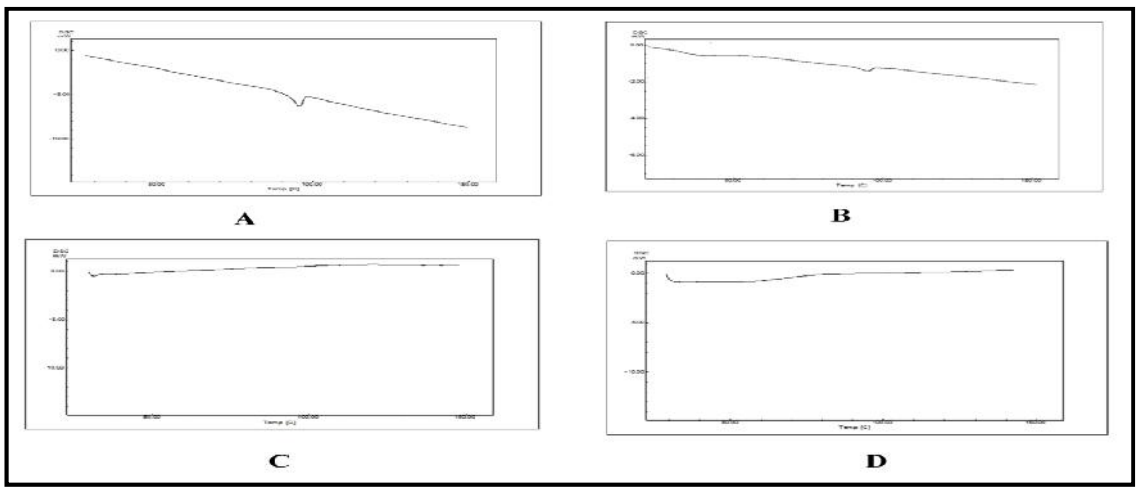

Figure 6.2 DSC thermogram of optimization of LPV loading in MCM-48NPs LPV: MCM-48NPs (A) 1:1 (B) 1:1.25 (C) 1:1.5 and (D) 1:2

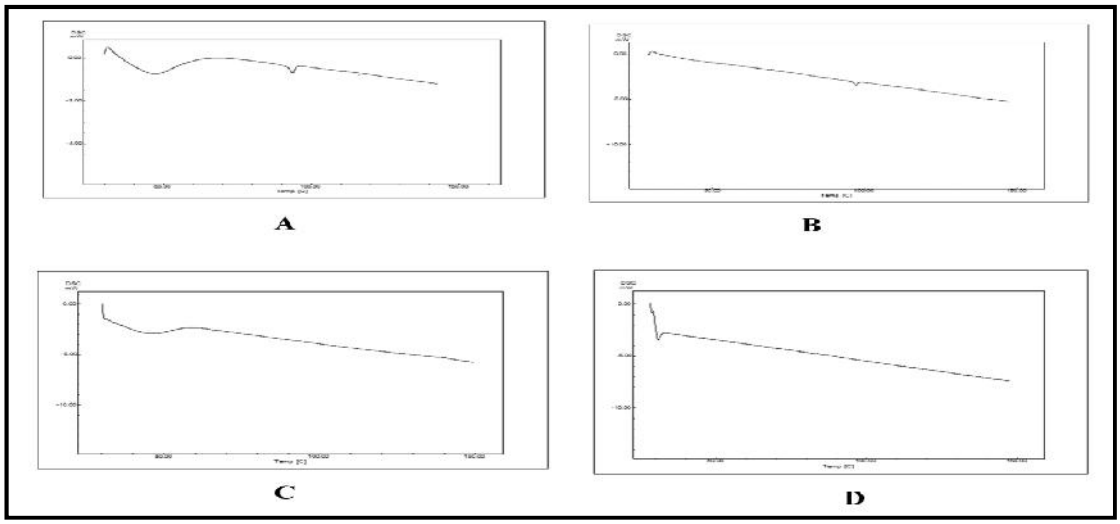

Figure 6.3 DSC thermogram of optimization of LPV loading in MCM-41NPs LPV: MCM-41NPs (A) 1:1 (B) 1:1.25 (C) 1:1.5 and (D) 1:2

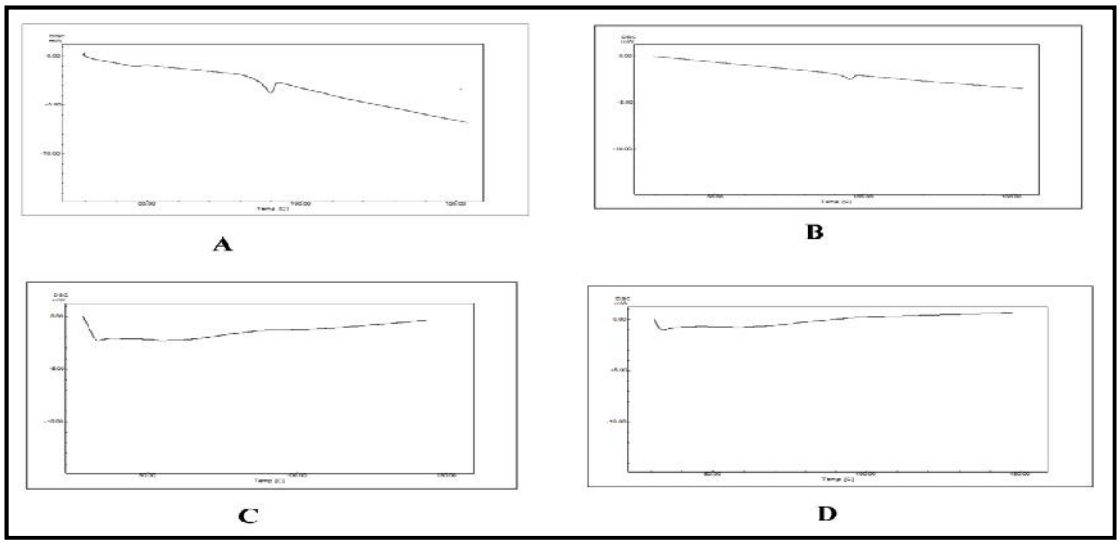

Figure 6.4 DSC thermogram of optimization of LPV loading in SBA-15NPs LPV: SBA-15NPs (A) 1:1 (B) 1:1.25 (C) 1:1.5 and (D) 1:2

6.13.2 Thermogravimetric Analysis

TGA thermograms were obtained to evaluate and further confirm the loading (wt %) of the LPV in MCM-48NPs, MCM-41NPs and SBA-15NPs. In Fig 6.5 TGA thermogram of LPV and L-MCM-48NPs, L-MCM-41NPs and L-SBA-15NPs show their stepwise weight loss. The thermogram in Fig. 6.5 A shows that LPV remain unchanged until the temperature of analysis reaches 230 °C. Then there was a gradual weight loss between 230 to 350 °C and a between 360 to 550 °C, that shows ultimate LPV decomposition. Fig 6.5 C, R-MCM-48NPs shows thermal behaviour of initial reduction in weight between 230 to 380°C that was assign to initial weight loss and a second between 390 to 530°C because of ultimate LPV decomposition.

The stable line after 530°C in thermogram because only silica nanoparticles were remained. Based on the %weight loss, the loading capacity of MCM-48NPs was determined to be 49%. The same results were found for MCM-41NPs and SBA-15NPs respectively in Fig 6.5 B and D and it shows loading capacity 40% and 57% on the basis of % weight loss of LPV. Therefore TGA and UV spectroscopy showed almost same results of LPV loading in different carrier and results are shown in table 6.4

Table 6.4 Drug loading efficiency results for L-MSNs by two different Method

Drug loading (% loading)	UV Method	TGA Method
MCM-48	46.83%	49%
MCM-41	38.72%	40%
SBA-15	54.14%	57%

The reason for differences in loading capacity of carriers is same as given in section 5.13.2 After confirming the LPV was loaded in MCM-48NPs, MCM-41NPs and SBA-15NPs, it were designated as L-MCM-48NPs, L-MCM-41NPs and L-SBA-15NPs

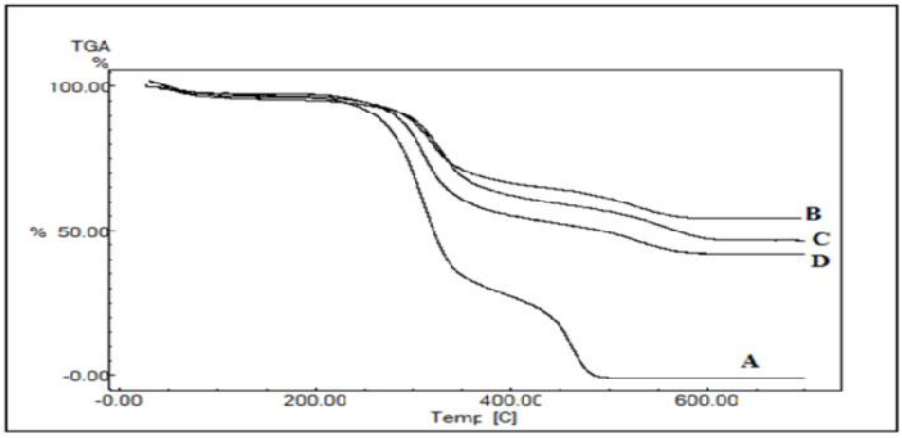

Figure 6.5 TGA Thermogram of (A) LPV, (B) L-MCM-41NPs, (C) L-MCM-48NPs and (D) L-SBA-15NPs

6.14 Characterization and Evaluation of L-MCM-48NPs, L-MCM-41NPs and L-SBA-15NPs (L-MSNs)

L-MCM-48NPs, L-MCM-41NPs and L-SBA-15NPs (L-MSNs) were characterized and evaluated for their intact mesoporous nature of nanoparticles and for drug loading. For evaluation different instrumental techniques were used that are described below.

6.14.1 Transmission electron microscopy (TEM)

The L-MSNs samples were analyzed by TEM. The TEM images confirmed that, mesoporous structure of MCM-48NPs, MCM-41NPs and SBA-15NPs was as such after LPV loading, that is showing in Fig 6.6 A, B and C respectively. Dark spots were observed in TEM image of L-MSNs that confirmed the LPV molecules were present with in mesopores.

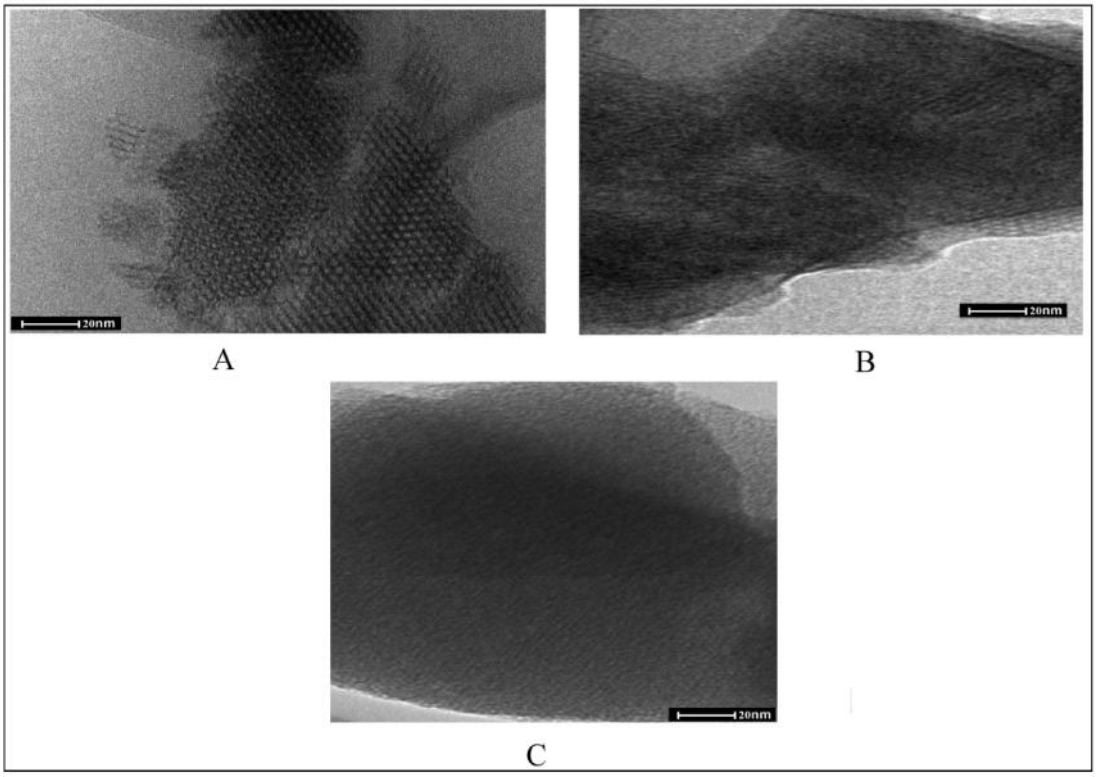

Figure 6. 6 After LPV loaded in (A) MCM-48NPs, (B) MCM-41NPs and (C) SBA-15NPs

6.14.2 FTIR analysis

For functional group identification and confirming the compatibility between LPV and silica nanoparticles, FT-IR study was carried out. FT-IR spectra of pure LPV is shown in Fig 6.7. The LPV spectrum shows peaks at peaks at 1660.86 cm-1 relative to C=O stretching aliphatic aldihydic group, peak at 3061.03cm-1 relative to OH stretch hydrogen bonded acidic group, and peak at 3386.74 cm-1 relative to NH stretching Amidic group. That confirm the obtained sample was lopinavir. The FT-IR spectrum of MCM-48NPs, MCM-41NPs and SBA-15NPs are shown in Fig 5.11.2 that show a broad peak between 3350-3500 cm^{-1} that indicate the presence of isolated terminal silanol groups. The Si-O-Si and Si-OH stretching vibrations are shown at 1084 and 801 cm-1 respectively. In Fig 6.8 A, L-MCM-48NPs-PM

spectrum show characteristic peaks of LPV and MCM-48NPs which proves compatibility between both drug and silica nanoparticles. Similar results were obtained for L-MCM-41NPs-PM and L-SBA-15NPs-PM that are shown in Fig 6.8 B and C. On the other hand, in Fig.6.9 A, B and C, L-MCM-48NPs, L-MCM-41NPs and L-SBA-15NPs spectra show a remarkable decrease of the peak at 1660.86 cm-1, 1706 cm-1 and disappearance of other major peaks of LPV, indicating the complete uptake of the LPV by mesoporous silica nanoparticles. These changes also suggest that the isolated terminal silanol group present in mesoporous silica nanoparticles have some interactions with LPV functional groups.

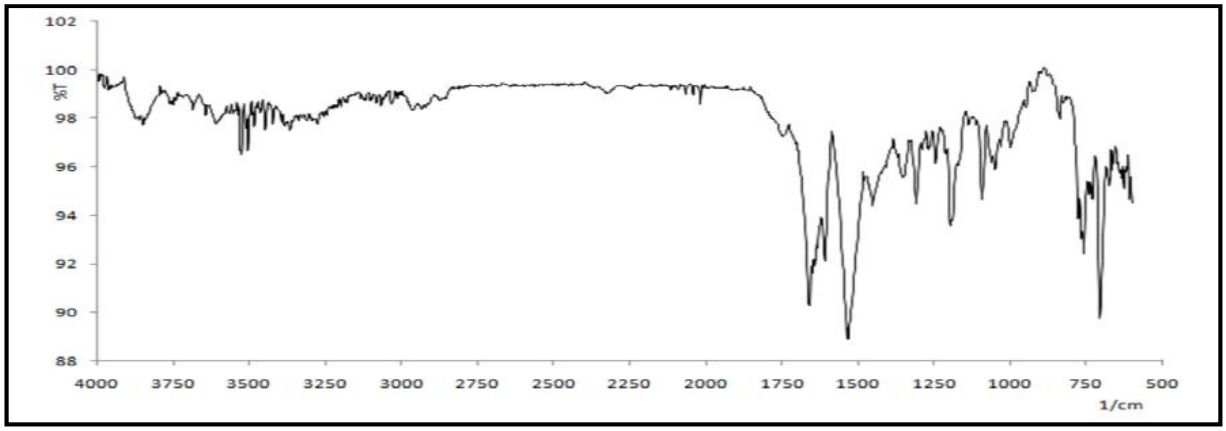

Figure 6.7 FT-IR spectra of LPV

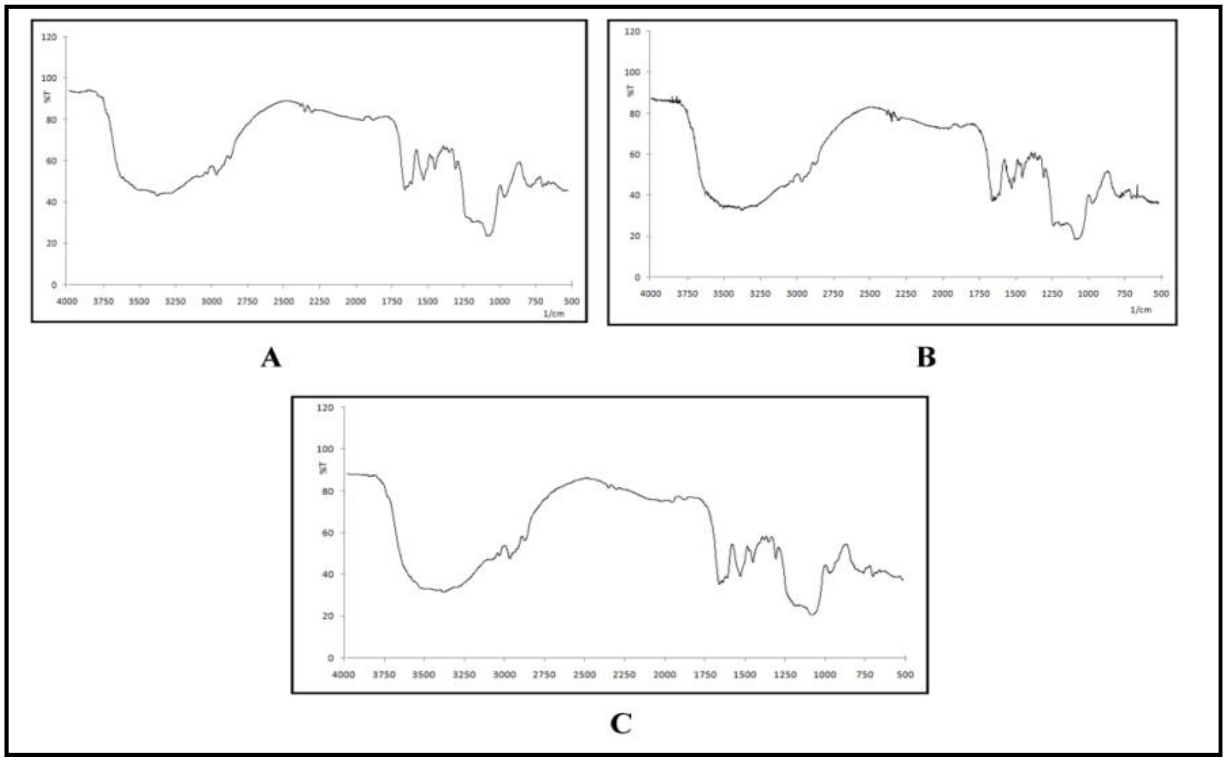

Figure 6.8 FT-IR spectra of physical Mixture of (A) LPV+MCM-48NPs, (B) LPV+MCM-41NPs and (C) LPV+SBA-15NPs

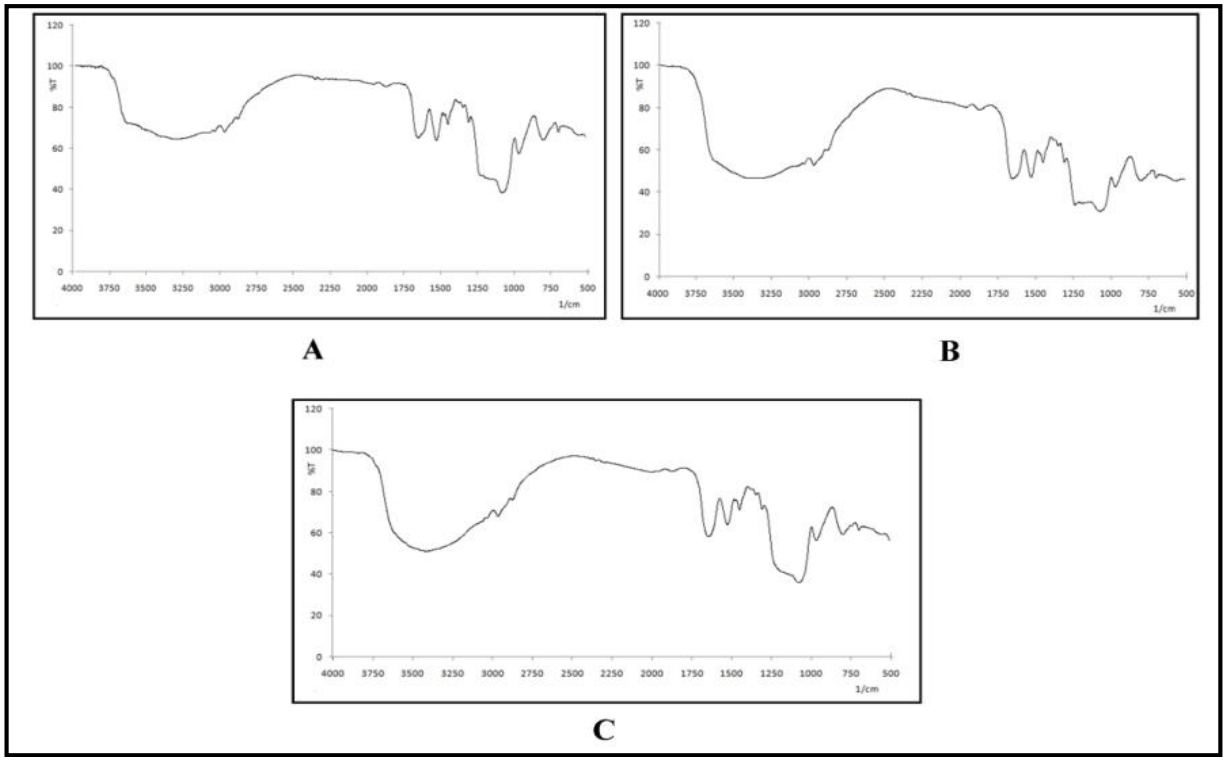

Figure 6.9 FT-IR spectra of (A) L-MCM-48NPs, (B) L-MCM-41NPs and (C) L-SBA-15NPs

6.14.3 Differential Scanning Calorimetry (DSC)

The DSC thermogram of crystalline pure LPV, MCM-48NPs, physical mixture of LPV and MCM-48 and L-MCM-48NPs are shown in Fig.6.10 A. Crystalline LPV thermogram exhibited a sharp endothermic peak at 94°C which corresponds to its fusion point showing in Fig 6.10(A) A. Fig 6.10(A) B shows MCM-48NPs thermogram, that did not show any transition because the fusion point of silica is very high. In physical mixtures, the sharp endothermic peak of LPV was present indicating the compatibility between MSNs and pure LPV that showing in Fig 6.10(A) C. Fig 6.10(A) D did not show any sharp endothermic peak of LPV in L-MCM-48NPs. The same results were found for MCM-41, L-MCM-41NPs-PM, L-MCM-41NPs and SBA-15, L-SBA-15NPs-PM, L-SBA-15NPs in Fig 6.10(B) and Fig 6.10(C) Respectively. These all results suggested that, no LPV was present on the outer surface of all MSNs (Fig. 6.10) that confirmed successful loading of LPV in nanoparticles.

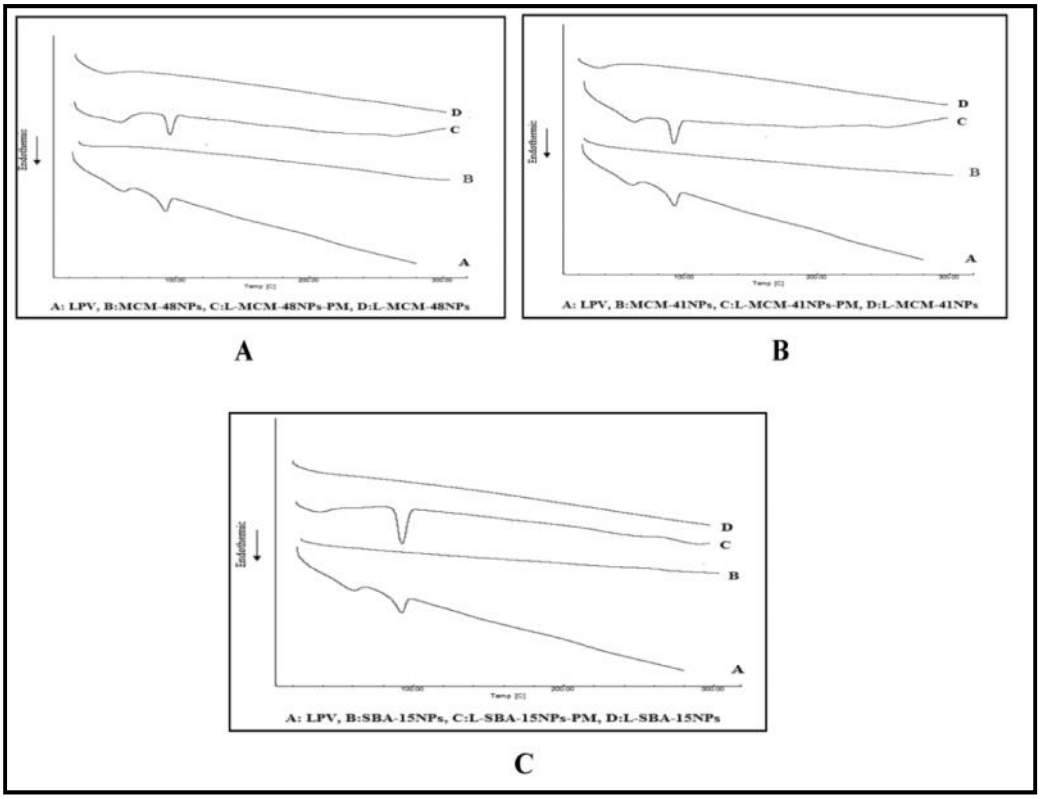

Figure 6.10 DSC Thermogram of (A) MCM-48NPs, (B) MCM-41NPs and (C) SBA-15NPs

6.14.4 Powder X-ray diffraction (XRD)

The intactness of mesopores structure of the MCM-48NPs, MCM-41NPs and SBA-15NPs after LPV loading was again confirmed by S-PXRD. S-PXRD patterns were studied after the loading process. Before LPV loading MCM-48NPs, MCM-41NPs and SBA-15NPs diffractogram showed typical reflections pattern between 0.5° to10° that was shown in Fig 5.5 A, B and C (chapter 5, section 5.11.3) respectively. The same diffraction patterns with decrease intensity of peaks in MCM-48NPs, MCM-41NPs and SBA-15NPs were observed in Fig 6.11 A, B and C, after LPV loading confirming the mesoporous structure was intact after drug loading. The wide angle P-XRD pattern of pure LPV and L-MCM-48NPs, L-MCM-41NPs and L-SBA-15NPs are shown in Fig 6.12 a, b, c and d. The wide angle powder XRD pattern of pure LPV showed several characteristic peaks at region 5-40° in the 2θ/5s region, which confirmed the crystalline nature of the LPV. The LPV loaded MCM-48NPs, MCM-41NPs and SBA-15NPs did not show these LPV characteristic peaks in W-PXRD pattern confirming that the LPV was completely loaded in nanoparticles and no crystalline drug remained on the outer surface of nanoparticles respectively.

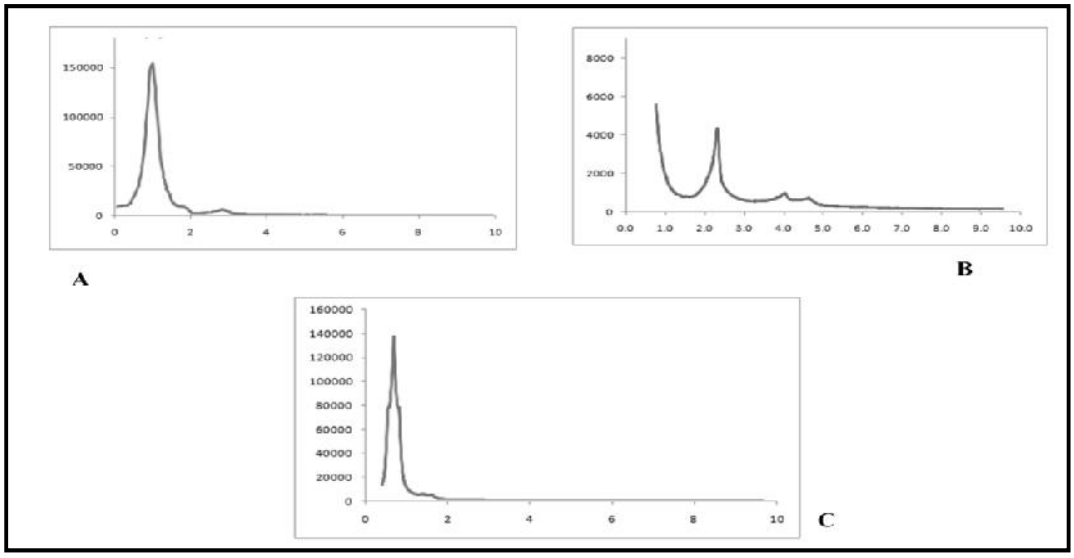

Figure 6.11 S-PXRD (A) L-MCM-48NPs, (B) L-MCM-41NPs and (C) L-SBA-15NPs

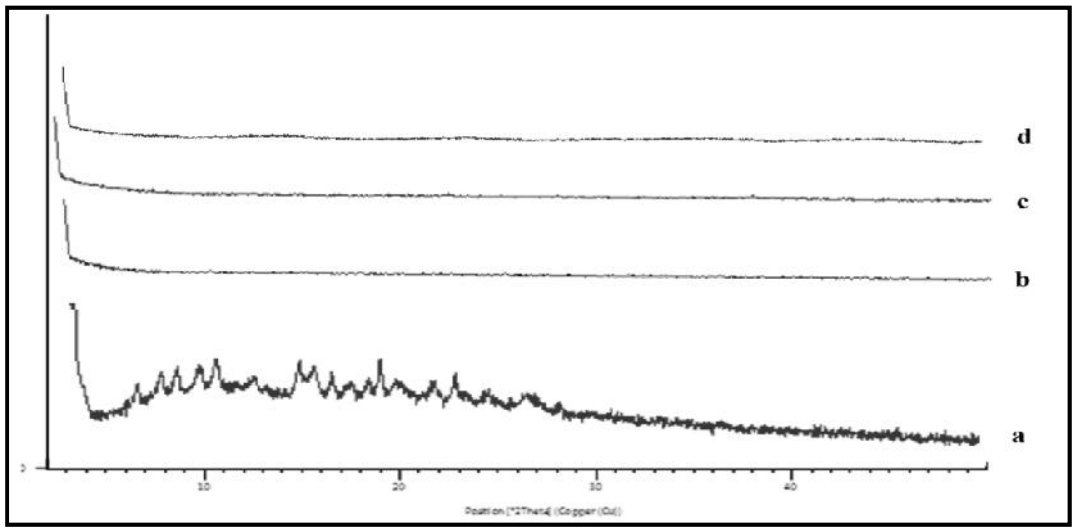

Figure 6.12 W-PXRD (a) LPV (b) L-MCM-48NPs, (c) L-MCM-41NPs and (d) L-SBA-15NPs

6.14.5 Nitrogen adsorption isotherm (BET surface analysis)

To confine the LPV molecules present inside or just present outside the surface of MSNs nitrogen adsorption-desorption study was carried out to find out the place of drug molecules. The nitrogen adsorption desorption isotherms were obtained to determine the pore size and pore volume of MSNs [6,7] before and after the drug loading.

The pore volume and surface area are usually decreased as a consequence of the MSNs–drug interaction. The results shows pore volumes of MSNs were decreases after LPV molecule loaded. Decrease in pore volume confirms drug molecules present inside the pores of nanoparticles.

Nitrogen adsorption-desorption isotherms of MCM-48NPs, MCM-41NPs and SBA-15NPs were shown in Fig.5.6 (Chapter 5 Section 5.11.4) and after the LPV loaded in MCM-48NPs, MCM-41NPs and SBA-15NPs, it shows typical type IV isotherm in Fig 6.13 A,B and C according to IUPAC classification of isotherms.

The calculated BET specific surface area, pore size and pore volume for MCM-48NPs, MCM-41NPs and SBA-15NPs and L-MCM-48NPs, L-MCM-41NPs and L-SBA-15NPs were given in Fig. 6.14 and table 6.4. Numerical data shows decrease in surface area, pore volume and pore size of MSNs after the LPV was loaded and that proves the drug molecule was totally entrapped in mesopores of nanoparticles.

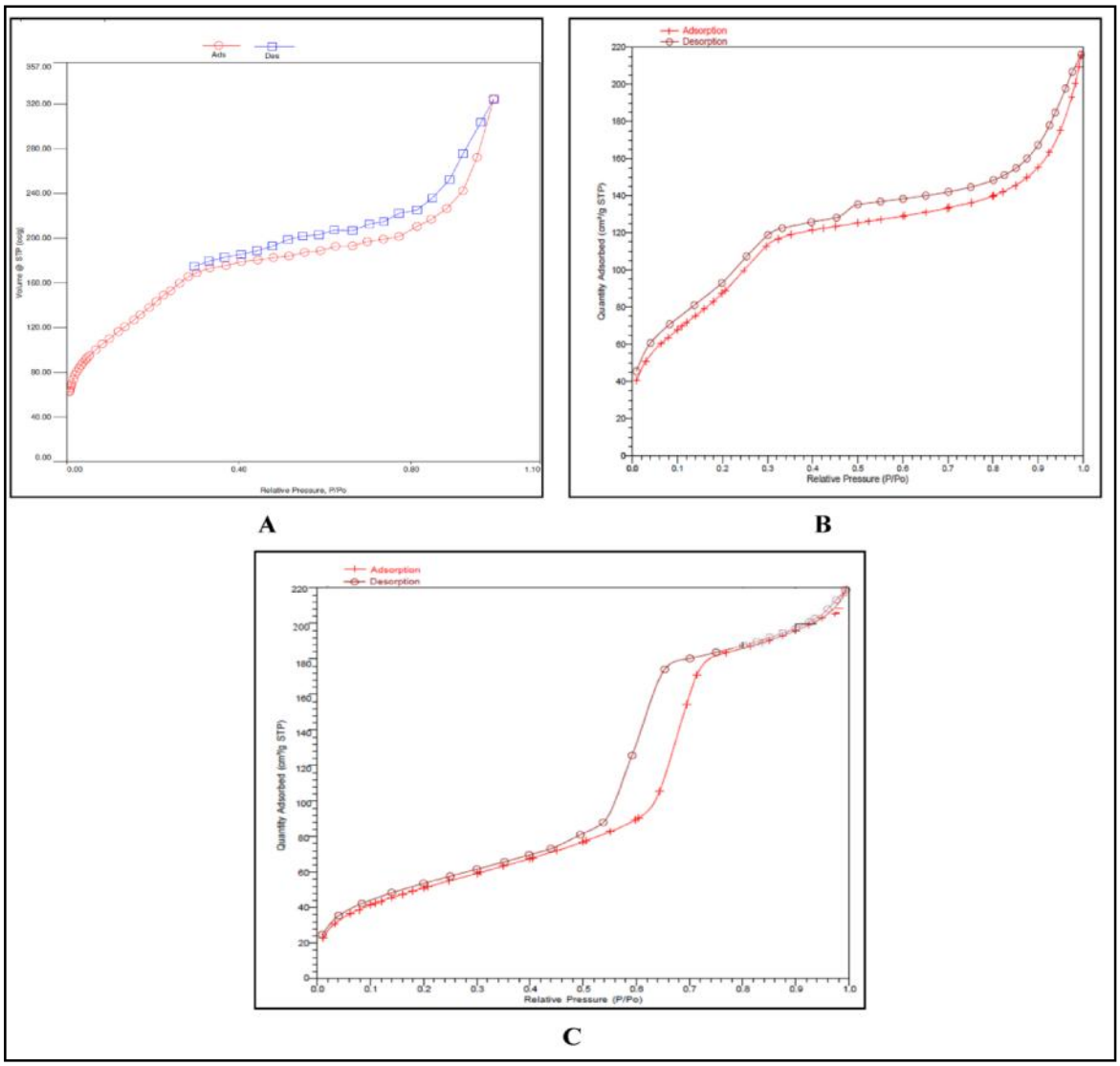

Figure 6.13 N2 Adsorption desorption isotherms of (A) L-MCM-48NPs, (B)L-MCM-41NPs and (C) L-SBA-15NPs

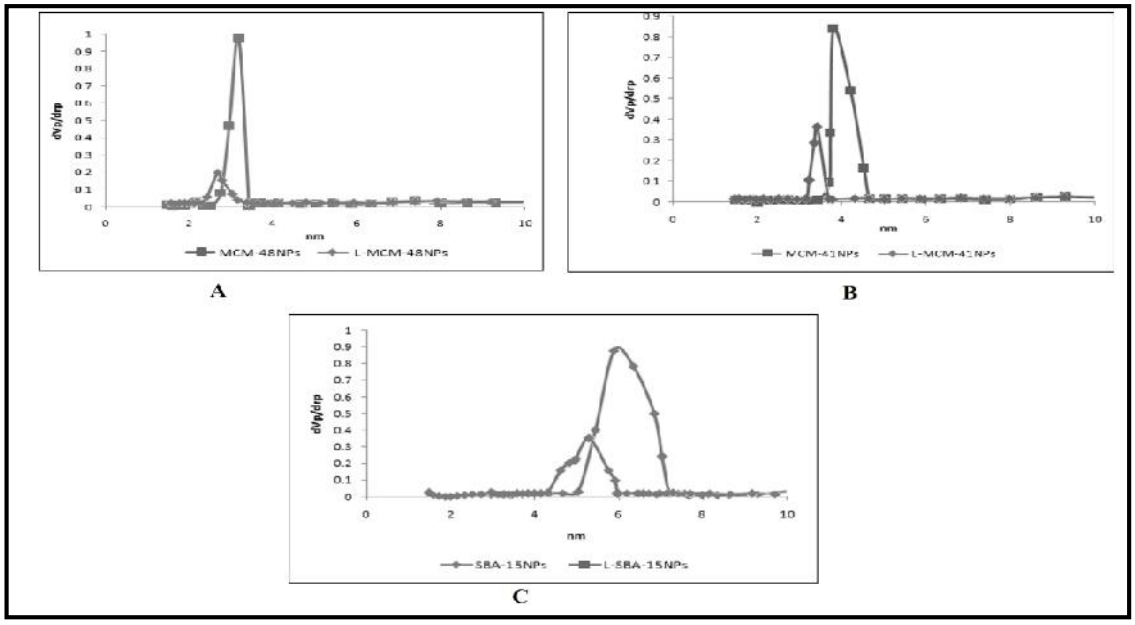

Figure 6.14 Pore size after LPV loading in (A) MCM-48NPs, (B) MCM-41NPs and (C) SBA-15NPs

Table 6.5 BET surface area Pore diameter and volume of MCM-48NPs, MCM-41NPs and SBA-15NPs before and after LPV loading

Name of compound	BET surface area	Pore volume	Pore diameter
MCM-48NPs	1220.29 m^2/g	0.96cm^3/g	3.2nm
L-MCM-48NPs	405.87 m^2/g	0.25 cm^3/g	2.8nm
MCM-41NPs	935.46 m^2/g	0.82cm^3/g	3.9nm
L-MCM-41NPs	345.55 m^2/g	0.36 cm^3/g	3.5nm
SBA-15NPs	880.66 m^2/g	0.89cm^3/g	5.9nm
L-SBA-15NPs	293.65 m^2/g	0.32 cm^3/g	5.3nm

6.15 Tablet Formulation of L-MCM-48NPs, L-MCM-41NPs and L-SBA-15NPs (L-MSNs)

Lopinavir (200 mg) content tablet from L-MSNs were prepared by same procedure and excipients which is mention in section 6.5. Prepared tablets were evaluated by various parameters such as weight variation, hardness, friability and disintegration time etc. The results are showing in Table 6.6.

Table 6.6 Evaluation of Prepared L-MCM-48NPs, L-MCM-41NPs and L-SBA-15NPs Tablets

Parameters	L-MCM-48NPs	L-MCM-41NPs	L-SBA-15NPs
Hardness kP	8-11 kP	8-11 kP	8-11 kP
Friability (%)	< 1 %	< 1 %	< 1 %
Disintegration time (Min)	2±0.2 min	3±0.3 min	2±0.3 min
Weight variation (mg)	750 ±6.88	750.35 ±5.88	750.62 ±7.38
Drug content (%)	98.12-101.56%	98.55-100.56%	99.12-100.36%

6.15.1 Tablet Formulation of L-MSNs and R-MSNs

Lopinavir/Ritonavir (200/50 mg) content tablet from L-MSNs/R-MSNs were prepared by same procedure and excipients which were mention in section 6.5. Prepared tablets were characterized by various parameters such as weight variation, hardness, friability and disintegration time etc. The results are showing in Table 6.7.

Table 6.7 Evaluation of Prepared LR-MCM-41NPs and LR-MCM-48NPs Tablets

Parameters	LR-MCM-48NPs	LR-MCM-41NPs	LR-SBA-15NPs
Hardness kP	9-12 kP	9-12 kP	9-12 kP
Friability (%)	< 1 %	< 1 %	< 1 %
Disintegration time (Min)	2±0.2 min	3±0.3 min	2±0.3 min
Weight variation (mg)	903.12 ±6.88	899.45 ±7.88	902.26 ±6.38
Drug content (%)	98.12-101.56%	98.55-100.56%	99.12-100.36%

MF for Lopinavir/ritonavir as available in film coated tablet with dose 200/50mg of LPV/RTV.

6.16 *In-vitro* dissolution study of LPV

In-vitro dissolutions were carried out at different pH with using minimum amount of surfactant was used in order to study the release profile of drug in different regions of GI tract. LPV dissolution from different MSNs were compared with pure crystalline LPV and MF of LPV/RTV. Drug release studies were performed to see the release pattern of pure LPV and drug loaded mesoporous silica nanoparticles in 0.1 N HCl with 0.75 % polyoxyethylene 10 lauryl ether (PLE), Acetate buffer pH 4.5 with 0.75 % PLE and Phosphate buffer pH 6.8 with 0.75 % PLE. The dissolution rate was significantly enhanced in the L-MCM-48NPs, L-MCM-41NPs and L-SBA-15NPs as compared to pure LPV. As per IP the dissolution media is 900 ml of a solution prepared by dissolving 15.7g of polyoxyethylene 10-lauryl ether (PLE) in 0.1 M solution of hydrochloric acid. PLE is surfactant use for enhancing the solubility of LPV and as per FDA minimum amount of surfactant can be use for the dissolution study as per requirement in developed formulation. The augment in dissolution rate in silica nanoparticles was observed, because of the conversion of crystalline LPV in amorphous form after loading into mesoporous nanoparticles. The LPV release profiles of L-MCM-48NP and L-SBA-15NPs showed more than 95% drug release in all dissolution media within 45 min, whereas L-MCM-41NP showed

almost 56.3 %, 59.7% and 66.5% drug release in 0.1 N HCl with 0.75 % PLE, acetate buffer pH 4.5 with 0.75 % PLE and phosphate buffer pH 6.8 with 0.75 % PLE respectively. Pure LPV and LPV/RTV MF did not achieve complete dissolution in any of the selected media over the test period of 60 min. LPV was incorporated into the mesopores of nanoparticles that change the crystalline nature of LPV in an amorphous form that improves the solubility rate and dissolution[8-11] of LPV. In dissolution profile of LPV, L-MCM-48NPs showing better dissolution profile than L-MCM-41NPs is might be due to small pore size of nanoparticles and the high surface area. Because of high surface area it adsorbs more drug molecule very efficiently. The LPV molecules adsorbed in the high surface of the 3D interconnected MCM-48NPs gave rapid diffusion and faster dissolution in the dissolution media while, MCM-41NP has cylindrical pore 2D hexagonal structure, appeared to restrict the drug molecules in the pore channels from diffuse into the dissolution media that gives slow drug release.[12,13] L-SBA-15NPs also shows more than 90% dissolution of LPV in all dissolution media, the reason of SBA-15NPs showing better dissolution profile than MCM-41NPs, is might be due to high amount of silanol group present in SBA-15NPs than MCM-41NPs that adsorb more amount of LPV molecules and also SI-OH groups on SBA-15NPs form very weak bonding with LPV molecules as compared to MCM-41NPs, that can be easily and quickly broken down in dissolution media.[14,15] Therefore because of all these reasons While comparing dissolution rate from L-SBA-15NPs and L-MCM 48NPS, it was almost similar with slight faster drug release from L-SBA-15NPs.

The graphical representation of release profile of LPV from pure LPV, develop formulation of LPV with various mesoporous silica nanoparticles and MF in different dissolution media shown in Fig 6.15.

Fig 6.15 and 6.16 shows LPV/RTV formulation (LR-MSNs) did not show any major difference in dissolution profile of LPV as compare to L-MSNs in all dissolution media respectively. The result shows RTV did not show any role in in-vitro dissolution study of LPV.

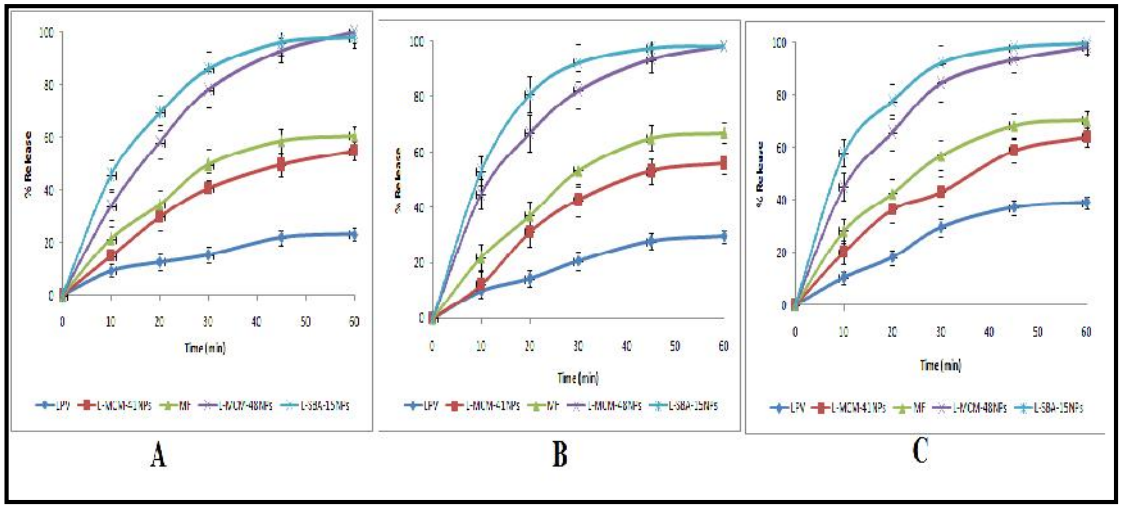

Figure 6.15 Release profile of LPV from pure LPV, develop formulation of LPV with various mesoporous silica nanoparticles and marketed formulation in (A) 0.1N HCl with 0.75 % PLE; (B) pH 4.5 acetate buffer with 0.75% PLE; (C) pH 6.8 phosphate buffer with 0.75% PLE

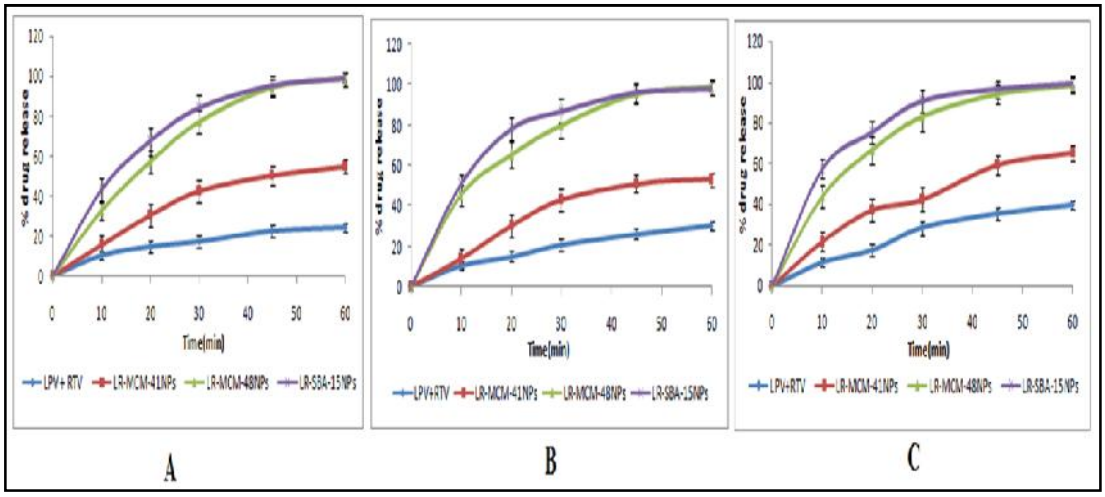

Figure 6.16 Release profile of LPV from combination of LPV/RTV, LR-MSNs and MF in (A) 0.1N HCl with 0.75 % PLE; (B) pH 4.5 acetate buffer with 0.75% PLE; (C) pH 6.8 phosphate buffer with 0.75% PLE

6.17 In-vivo study of LPV

LPV is a typical BCS II drug; whose absorption affected by the poor solubility in GI tract and widely metabolized by CYP3A4[16, 17]. In this study, the results of in-vitro dissolution studies were confirming the enhanced dissolution of LPV by L-MCM-48NPs, L-MCM-41NPs and L-SBA-15NPs compare to pure LPV. To study the silica nanoparticles effect, the in-vivo studies were performed in which the drug suspension was given orally to wistar rat. The results of plasma concentration-time profiles and the PK parameters of LPV are shown in Fig 6.17 and Table 6.7, respectively. In Fig. 6.17 it is clearly shown that the absorption rate of LPV in combined pure LPV/RTV was higher than alone pure LPV, when the combination of

pure LPV/RTV (20/5mg) administered orally it shows more plasma concentration of lopinavir (1.58±0.25µg/ml/hr) compare to the pure LPV (0.47±0.10 µg/ml/hr). The reason behind that is when Lopinavir administered alone, it rapidly metabolise in the liver by CYP3A5 and CYP3A4. Ritonavir a widely used as pharmacokinetic enhancer inhibits the CYP3A5 and CYP3A4 isoenzyme in the liver microsomes and therefore it increases the concentration of lopinavir in systemic circulation.[18-19] When L-MCM-48NPs, L-MCM-41NPs and L-SBA-15NPs administered orally in wistar rat, it shows slight enhancement in LPV plasma concentration, it was 0.81±0.19µg/ml/hr, 0.55±0.12µg/ml/hr and 0.75±0.16µg/ml/hr respectively but not more than the LPV concentration found in a combination of pure LPV/RTV. The reason behind that is same above. Also, LPV commercially available as the formulation is in the combination of lopinavir/ritonavir (200/50 mg). Therefore we also used combination tablet formulation of lopinavir/ritonavir loaded silica nanoparticles that were mention in section 6.5 and Table 6.2. Afterwards, to study the effect of the combination of LPV/RTV with different nanoparticles the in-vivo studies were performed in which the drug suspension was given orally to wistar rat. And in this study, the drug plasma concentration profile of LR-MCM-48Ps showed significant improvement in drug absorption as compared to pure LPV, the combination of pure LPV/RTV and MF of LPV/RTV. Area under concentration-time curve (AUC_{0-t}) of LPV was found 33.64±2.14µg/mL*h for LR-MCM-48NPs which was 9.37-fold, 3.18-fold and 1.63-fold higher with that of pure LPV (3.59±2.34 µg/mL*h), combination of LPV/RTV (10.57±3.23 µg/mL*h) and MF of LPV/RTV (20.57±2.22 µg/mL*h) respectively. The maximum peak plasma concentration (Cmax) of LPV was found 5.30±3.34µg/ml for LR-MCM-48Ps which was about 11.27-fold, 3.35-fold and 1.51-fold higher than that of pure LPV (0.47±0.10 µg/ml/hr), combination of LPV/RTV (1.58±0.25 µg/ml/hr) and MF of LPV/RTV (3.50±0.36 µg/ml/hr), respectively.

Likely Drug plasma concentration profile of LR-SBA-15NPs showed significant improvement in drug absorption compared to pure LPV, combination of pure LPV/RTV and MF of LPV/RTV. Area under concentration-time curve (AUC0-t) of LPV was found 31.95±2.14µg/mL*h for LR-SBA-15NPs which was 8.89-fold, 3.02 fold and 1.55-fold higher with that of pure LPV (3.59±2.34 µg/mL*h), combination of LPV/RTV (10.57±3.23 µg/mL*h) and MF of LPV/RTV (20.57±2.22 µg/mL*h)

respectively. The maximum peak plasma concentration (Cmax) of LPV was found 5.15µg/ml for LR-SBA15NPs which was about 10.95-fold, 3.25-fold and 1.47-folds greater than that of pure LPV (0.47±0.10 µg/ml/hr), combination of LPV/RTV (1.58±0.25 µg/ml/hr) and MF of LPV/RTV (3.50±0.36 µg/ml/hr), respectively.

Time to reach maximum plasma concentration (Tmax) for LR-MCM-48NPs, pure LPV, combination of pure LPV/RTV and MF of LPV was found to be 2.5 hours respectively. Half-life (t1/2) of LR-MCM-48NPs and LR-SBA-15NPs was compared with pure LPV, combination of pure LPV/RTV and MF of LPV/RTV, the t1/2 for LR-MCM-48NPs (3.95 ±0.32 h) and LR-SBA-15NPs (3.56±0.29 h) was not found much different than that of pure LPV (3.73±0.24 h), combination of pure LPV/RTV (3.72±0.19 h) and MF of LPV (3.38±0.26 h).

The enhancement in AUC and Cmax of LR-MCM-48NPs and LR-SBA-15NPs compared to pure LPV, combination of pure LPV/RTV and MF of LPV/RTV could be due to fast absorption of LPV by gastrointestinal wall, because of increased surface area and the reduced particle size followed by significantly improvement in dissolution rate, increased wettability and increase in adhesion surface area between nanoparticle and intestinal epithelium of villi which provides a direct contact with the absorbing membrane of the gut wall and also because of presence of RTV nanoparticles with the lopinavir nanoparticles, it inhibits the CYP3A4 and CYP3A5 isoenzyme in the liver and increased concentrations of lopinavir in blood circulation.

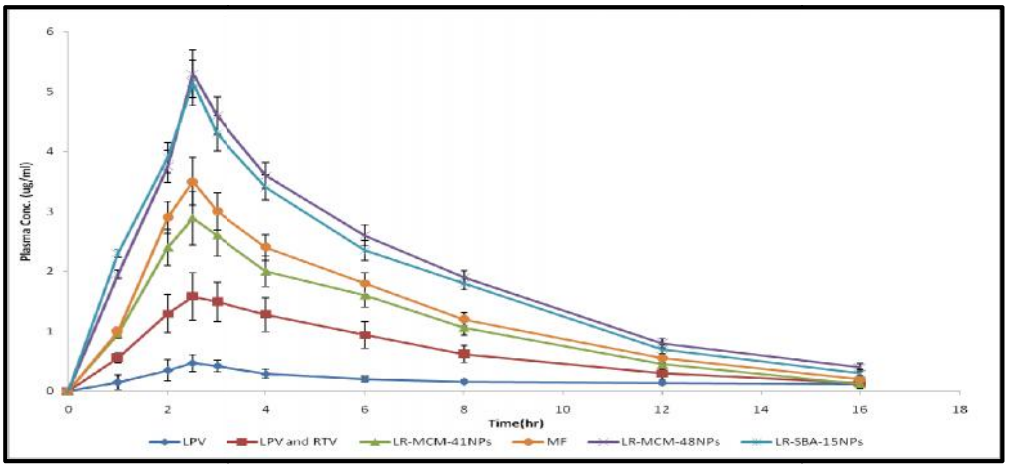

Figure 6.17 Graphical representation of LPV plasma profile for plain LPV, Combination of LPV/RTV, LR- MCM-41NPs, LR-MCM-48NPs, LR-SBA-15NPs and MF of LPV/RTV in Albino Wistar rat following oral administration

Table 6.8 Pharmacokinetic parameter of LPV with different MSNs

Parameter	Pure LPV	Pure LPV and RTV	LR-MCM-48 NPs	LR-MCM-41 NPs	LR-SBA-15NPs	MF
C_{max}	0.47±0.10 µg/mL	1.58±0.25 µg/mL	5.30±0.34 µg/mL	2.90±0.45 µg/mL	5.15 ±0.40 ug/mL	3.50±0.36 ug/ml
T_{max}	2.5 h	2.5h	2.5 h	2.5 h	2.5h	2.5 h
AUC_{0-t}	3.59±2.34 µg/mL*h	10.57±3.23 µg/mL*h	33.64±4.14 µg/mL*h	18.48±4.74 µg/mL*h	31.95±3.14 µg/mL*h	20.57±3.22 µg/mL*h
$T_{1/2}$	3.73±0.24 h	3.72±0.19 h	3.95±0.32 h	3.86±0.21 h	3.56±0.29 h	3.38±0.26 h

6.18 In vitro Cell Cytotoxicity Studies of L-MSNs (MTT Assay)

Cytotoxicity study of LPV, L-MCM-48NPs and L-SBA-15NPs was accomplished in Caco2 cells by mitochondrial activity (MTT assay) to assess the safety/tolerability of prepared formulation on viability of cells. As Caco2 cells were used as absorption model, the biocompatibility and tolerability assessment of LPV and L-MCM-48NPs, L-SBA-15NPs on absorption barrier was necessary. After 48 hr the % cell viability is more than 90 % at the concentration 500 µg/ml concentration of plain LPV and L-SBA 15 NPs, but slightly decrease the % cell viability in MCM-48NPs. (Fig. 6.18 A, B and C) The surface area and particle size of nanoparticles are important factors that affect the cell viability. The surface area of MCM-48NPs and SBA-15NPs was found to be 1220.29m2/g and 880.66 m2/g and pore size was 3.2nm and 5.9nm respectively. The avarage particle size of MCM-48NPs and SBA-15 NPs was around 100-200nm and 200-300nm respectively. It was found that small particle size and large surface area MCM-48NPs facilate more contact with cell than the large particle size and lower surface area[20-22] which may cause the slightly decrease the cell viability in MCM-48NPs. The results are showing in Fig 6.18. The result confirms the biocompatibility of mesoporous silica nanoparticles and its composition did not contribute intoxicity of caco-2 cell.

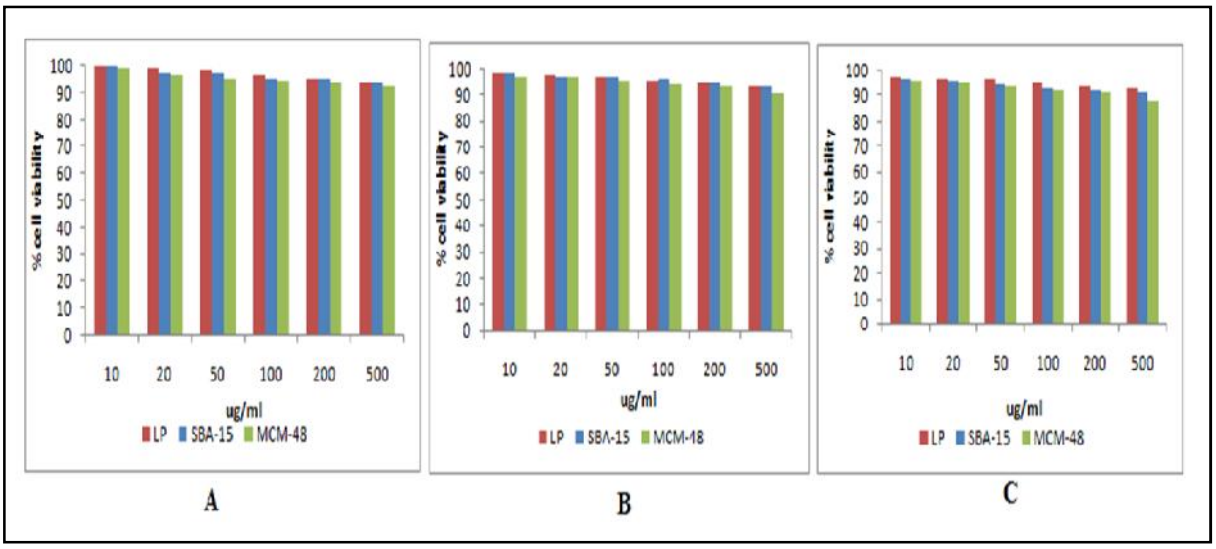

Figure 6.18 Cytotoxicity graphs for plain LPV and LPV loaded MCM-48NPs and SBA 15 NPs (A) 6hr (B) 24 Hr and (C) 48 Hr

Conclusion

In vitro cytotoxicity study of drug loaded MCM-48 and SBA-15 MSNs on Caco-2 cell as a function of concentration and incubation time was determined. The major difference in MCM-48NPs and SBA-15NPs was their surface morphology and chemistry. The results show that both the MSNs have different morphology and induced slight difference in in vitro cytotoxicity study. The slightly decrease in cell viability of caco-2 cell was more prominent when small size and larger surface area MCM-48 expose to higher concentration for longer duration of incubation. Under experimental condition it was found that both MSNs were biocompatible in drug delivery system.

6.19 Stability Study

6.19.1 Physical Stability

To verify the physical stability of L-MCM-48NPs, L-MCM-41NPs and L-SBA-15NPs (L-MSNs) at accelerated storage stability study was carried out.

When samples keep in accelerated storage condition there may be chances to changes in form of drugs by breaking the bonds between carrier and drug molecules. The changes were monitored by DSC and XRD analytical techniques, and MSNs structural stability was monitored by TEM analysis.

6.19.1.1 P-XRD study of L-MSNs after accelerated storage condition

Powder XRD patterns of L-MCM-41NPs, L-MCM-48NPs and L-SBA-15NPs (L-MSNs) are shown in Fig. 6.19 A, B and C respectively. L-MSNs samples were stored at 40°C ± 2°C/75% ± 5% relative humidity. The powder XRD patterns of all

samples were recorded after 1, 3 and 6 months. The powder XRD of L-MSNs was taken at angle 2θ in the range of 5–50º respectively and it did not shows any peaks relative to the crystalline LPV drug, that clearly indicated that LPV loaded in all MSNs are stable and not show any polymorphic change in drug.

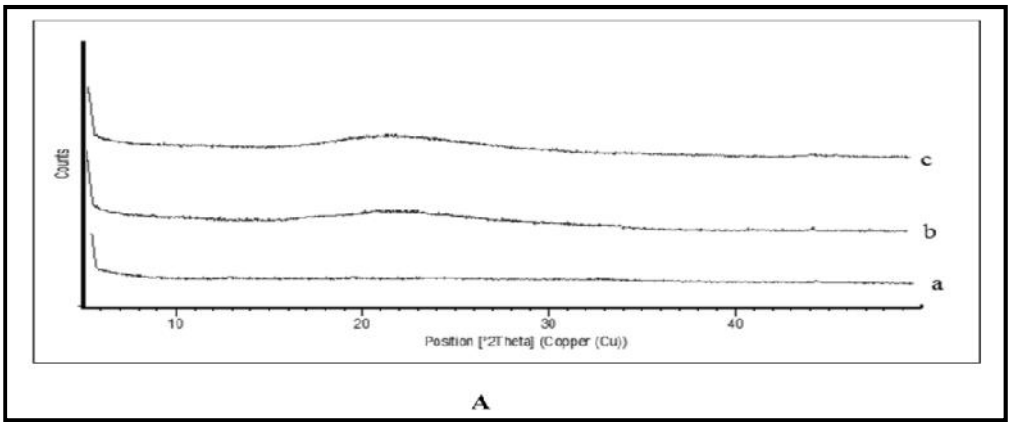

Figure 6.19 A: XRD pattern of L-MCM-41NPs in 40°C ± 2°C and 75% ± 5% relative humidity after A) 1 month B) 3 month C) 6 month

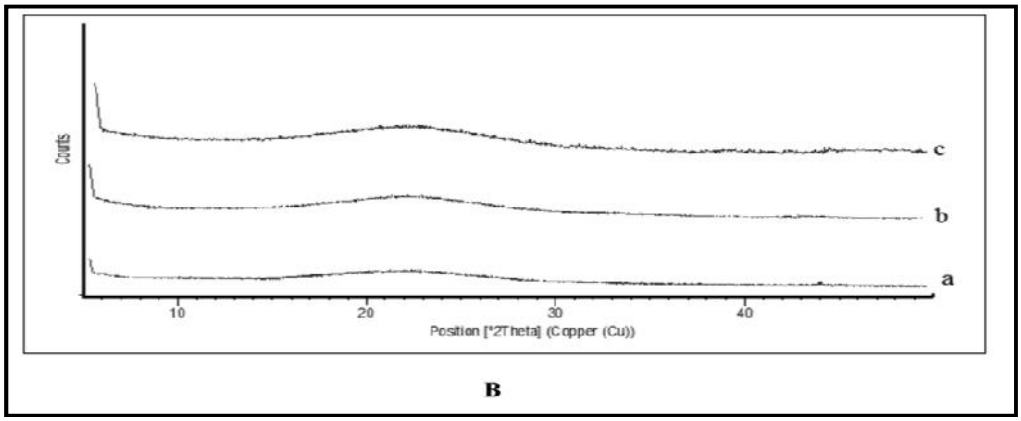

Figure 6.19 B: XRD pattern of L-MCM-48NPs in 40°C ± 2°C and 75% ± 5% relative humidity after A) 1 month B) 3 month C) 6 month

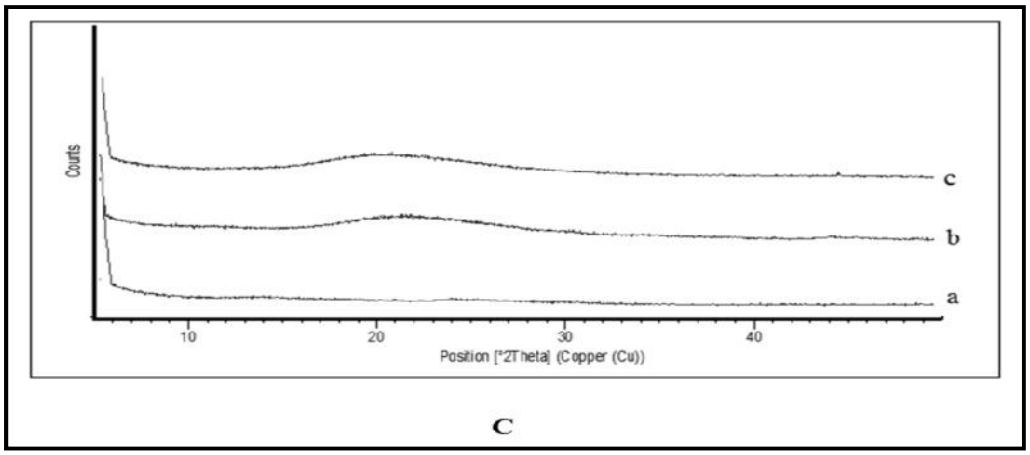

Figure 6.19 C: XRD pattern of L-SBA-15NPs in 40°C ± 2°C and 75% ± 5% relative humidity after A) 1 month B) 3 month C) 6 month

6.19.1.2 DSC study of L-MSNs after accelerated storage condition

DSC thermograms of L-MCM-41NPs, L-MCM-48NPs and L-SBA-15NPs (L-MSNs) are shown in Fig 6.20. L-MSNs samples were stored at 40 ◦C ± 2 ◦C and 75% ± 5% relative humidity. The DSC thermograms of all samples were recorded after storage of samples up to 1, 3 and 6 months. Fig 6.20 A, B and C shows DSC thermogram of L-MCM-41NPs, L-MCM-48NPs and L-SBA-15NPs at standard DSC condition respectively. The stability of LPV within MSNs was proved as LPV fusion peak could not be detected at any thermogram of DSC. In DSC Thermograms broad peak around 60°C recorded due to loss of humidity and no fusion peak was observed at fusion point of LPV around 94ºC, The absences of fusion peak of LPV indicate that the LPV was completely loaded and physically stable within the pores of MSNs.

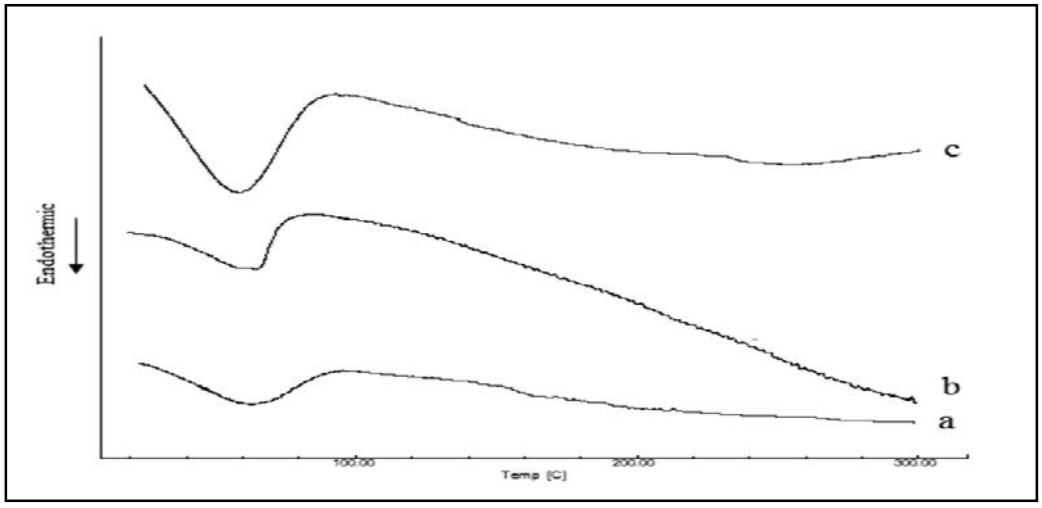

A

Figure 6.20 A: DSC of L-MCM-41NPs (A) 40°C ± 2°C/75% ± 5% relative humidity after a) 1 months b) 3 months c) 6 months

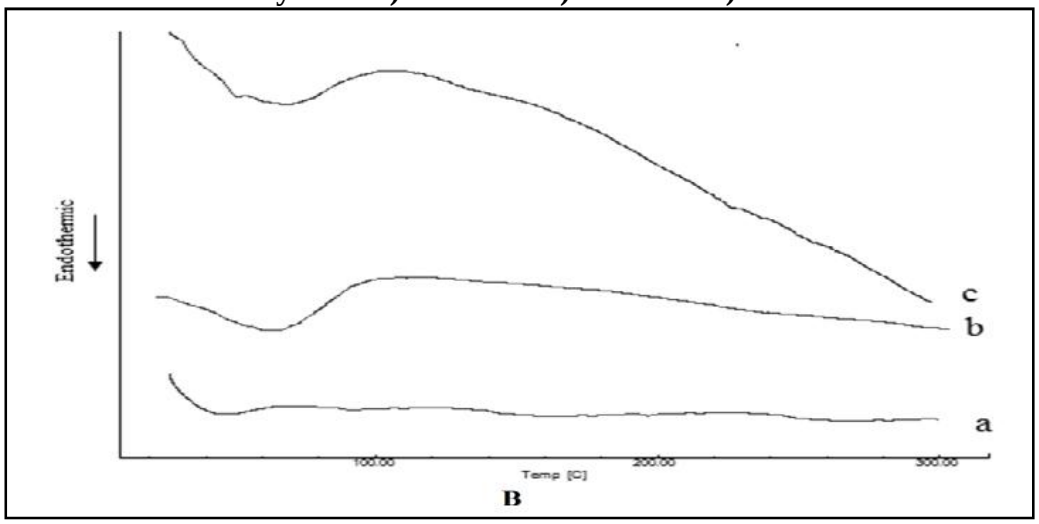

B

Figure 6.20 B: DSC of L-MCM-48NPs (A) 40°C ± 2°C/ 75% ± 5% relative humidity after a) 1 months b) 3 months c) 6 months

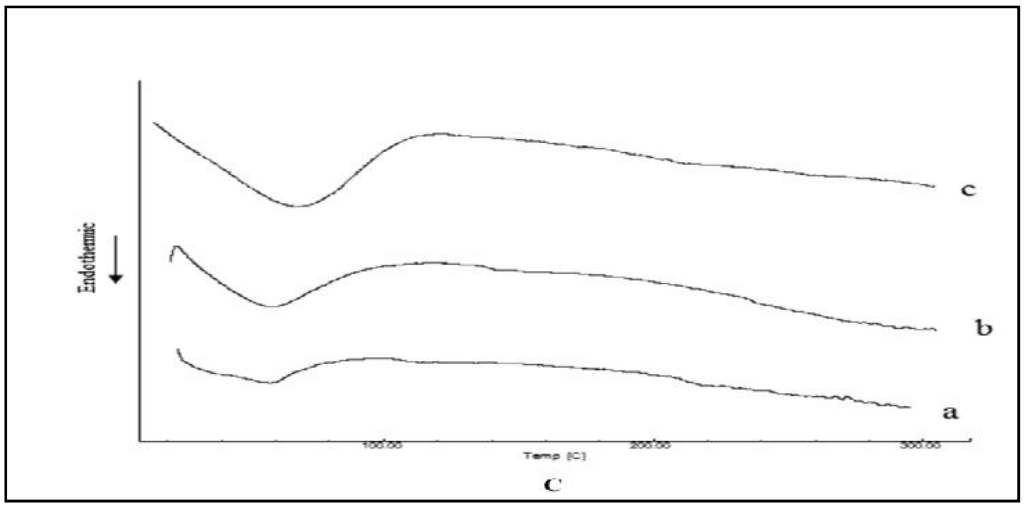

Figure 6.20 C: DSC of L-SBA-15NPs (A) 40°C ± 2°C/75% ± 5% relative humidity after a) 1 months b) 3 months c) 6 months

6.19.1.3 TEM study of L-MSNs after accelerated storage condition

The physical storage stability of L-MCM-41NPs, L-MCM-48NPs and L-SBA-15NPs (L-MSNs) respectively were checked by TEM images. The mesoporosity of L-MSNs were observed and checked individually after kept in accelerated stability condition for 1, 3 and 6 months. In all tested conditions all the drug loaded MSNs show good physical stability and found no structural changes in all MSNs. Fig 6.21 A, B and C revealed the structural integrity of L-MSNs after 1, 3 and 6 months at 40ºC ± 2ºC/ 75% ± 5% relative humidity respectively.

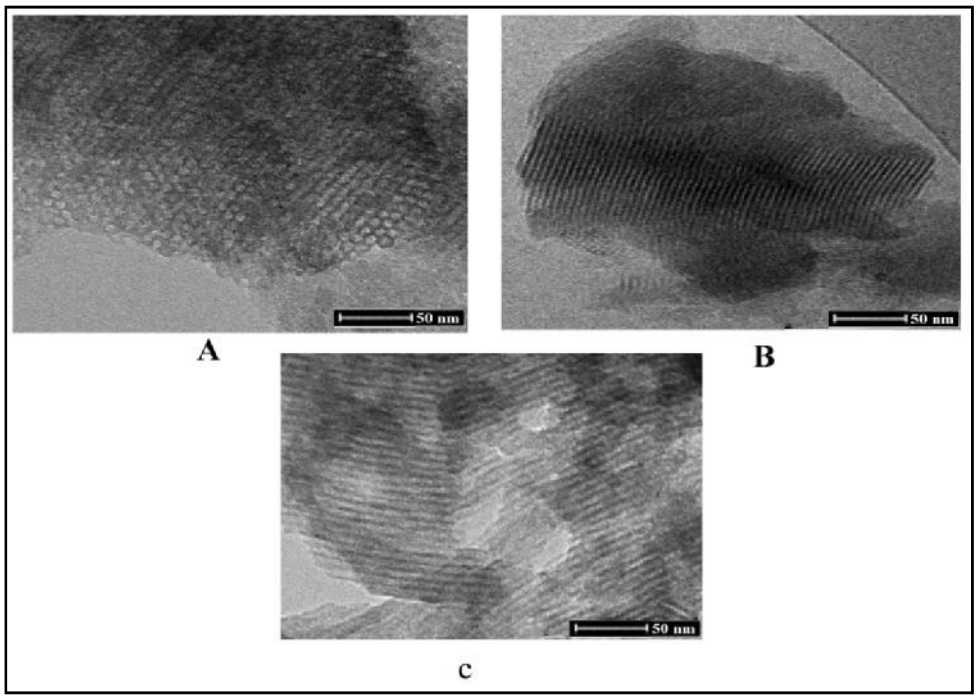

Figure 6.21 A: TEM images of L-MCM-41NPs in 40°C ± 2°C/75% ±5% relative humidity after A) 1 month B) 3 month C) 6 month

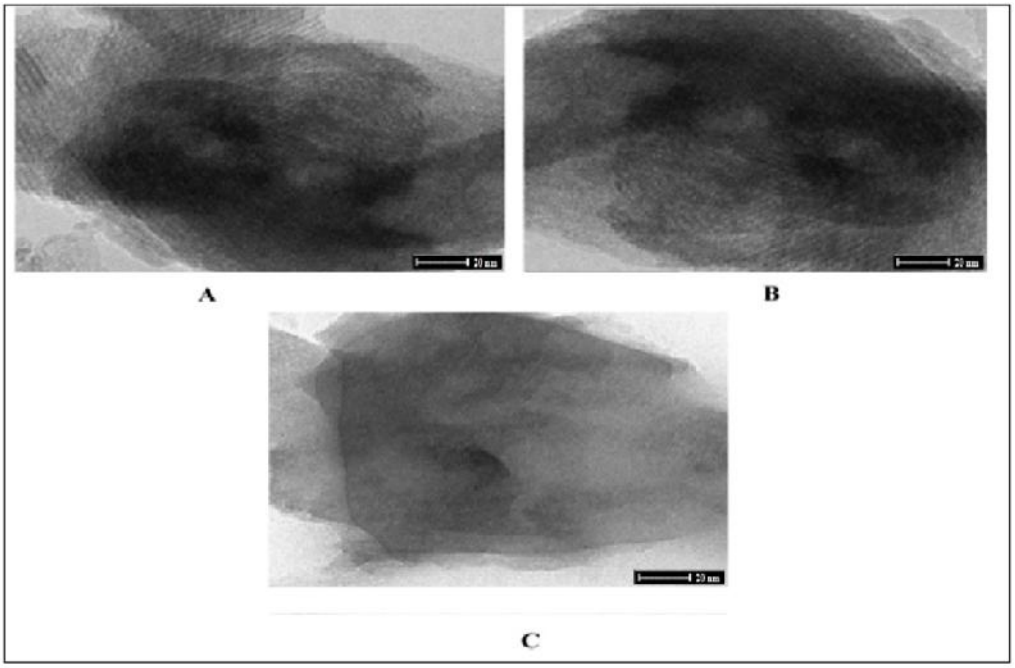

Figure 6.21 B: TEM images of L-MCM-48NPs in 40°C ± 2°C/75% ±5% relative humidity after A) 1 months, B) 3 months C) 6 months

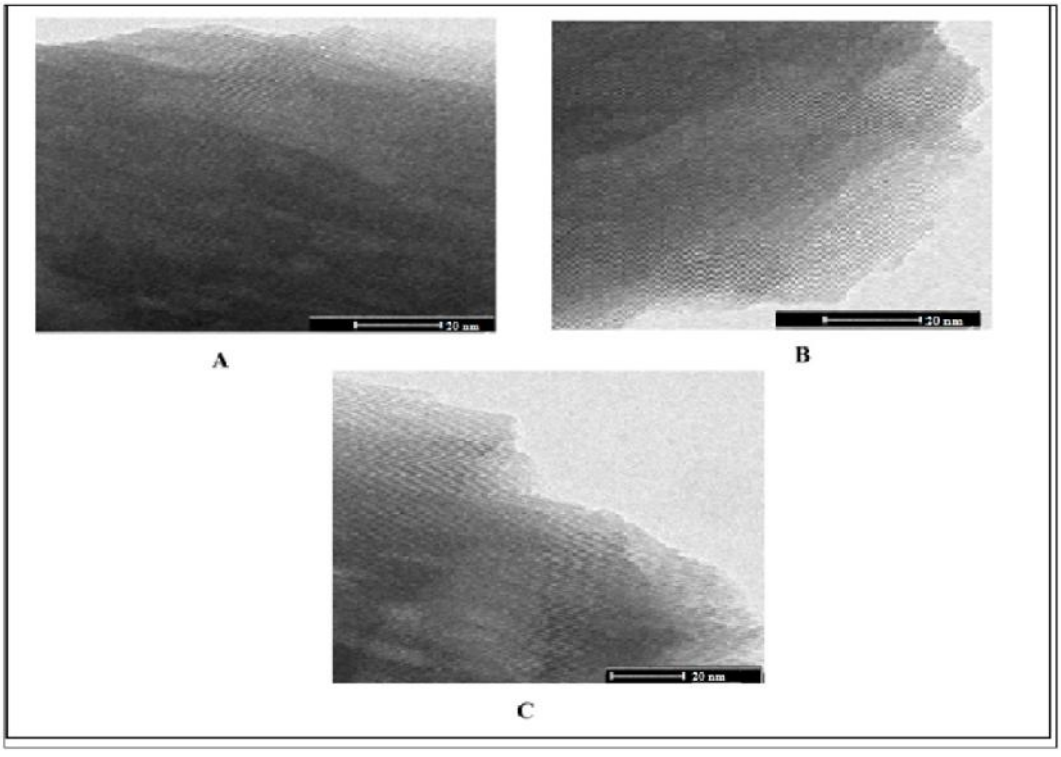

Figure 6.221 C: TEM images of L-SBA-15NPs in 40°C ± 2°C/75% ± 5% relative humidity after A) 1 months, B) 3 months C) 6 months

6.20.2 Chemical Stability

The Chemical stability of L-MCM-41NPs, L-MCM-48NPs and L-SBA-15NPs (L-MSNs) were checked by RP-HPLC. The chemical stability of drugs in MSNs was checked individually after kept in accelerated stability condition for 1, 3 and 6

months of samples. In all tested conditions all the drug loaded MSNs show good chemical stability and found no changes in content and concentration of drugs. The results are shown in table 6.9

Table 6.9 Chemical stability of L-MSNs (i.e. percentage drug content) at different time intervals, stored at 40°C ± 2°C/ 75% ± 5% relative humidity

Sr. No.	Time	40°C±2°C/75% ± 5% relative humidity	40°C±2°C/75% ± 5% relative humidity	40°C ± 2°C/75% ± 5% relative humidity
		% content of LPV in MCM-41NPs	% content of LPV in SBA-15NPs	% content of LPV in MCM-48NPS
1	Initial	100.88±0.20	101.90±0.37	100.12±0.79
2	1st Month	100.37±0.25	100.50±0.65	99.76±0.54
4	3rd Month	98.84±0.45	99.19±0.52	99.12±0.23
5	6th Month	98.40±0.23	98.39±0.34	98.08±0.65

Conclusion

It was evident from DSC, XRD and TEM studies show that MCM-41NPs, MCM-48NPs and SBA-15NPs are stable carriers for LPV. Although humidity and water absorbed on the surface of MSNs have possibility to affect the loaded drug in MSNs, but there were no crystallization changes and nucleation of drug occurred because of perfect match occurs between the drug molecule and MSNs pore diameter. Nucleation and crystallization of drug occur only when the diameter of carriers 20 times larger than the drug molecules. Therefore when drug molecule is perfectly enslaved in the pore of MSNs, its recrystaliization was prevented from both humidity and temperature.

Summery and Conclusion

In this study, the synthesized mesoporous silica nanoparticles MCM-41NPs, MCM-48NPs and SBA-15 were suitable carriers for poorly soluble LPV drug. LPV was loaded in all three silica nanoparticles to examine the effect of mesopores size and geometry on solubility through the drug loading. To achieve maximum drug loading, solvent evaporation method was preferred with an appropriate ratio of LPV and carrier (1:1.5). (L-MCM-48NPs, L-MCM-41NPs and L-SBA-15NPs) In addition, characterization results like DSC, PXRD and N2 adsorption-desorption confirmed that the LPV was successfully loaded into the mesoporous silica nanoparticles. In in-vitro drug dissolution study, MCM-41NPs MCM-48NPs and SBA-15NPs (MSNs) showed several advantages as a carrier for drug delivery respectively. All silica

carriers MCM-48NPs and SBA-15NPs could notably increase the dissolution rate of LPV as compared to the pure LPV, MCM-41NPs and LPV/RTV MF.

As Commercially LPV marketed formulation is available with the other protease booster namely Ritonavir (RTV). So we also prepare the formulation in combination of LPV/RTV using previously prepared RTV loaded MSNs to examine the effect of RTV on in-vitro and in vivo study. (LR-MSNs-NPs)

The dissolution study of LR-MSNs-NPs formulation did not show any major difference in dissolution profile of LPV in presence of RTV as compare to L-MSNs-NPs in all dissolution media respectively. That shows RTV did not show any role in in-vitro dissolution study of LPV.

In *in-vivo* assessment L-MCM-48NPs, L-MCM-41NPs and L-SBA-15NPs administered orally in wistar rat, it shows slight enhancement in LPV plasma concentration,it was 0.81±0.19µg/ml/hr, 0.55±0.12µg/ml/hr and 0.75±0.16µg/ml/hr respectively but not more than the LPV concentration 1.58±0.25µg/ml/hr found in a combination of pure LPV/RTV. It is clearly shown that the absorption rate of LPV in combined pure LPV/RTV was higher than alone pure LPV, when the combination of pure LPV/RTV administered orally it shows more plasma concentration of lopinavir compare to the pure LPV. The reason behind that is when Lopinavir administered alone, it rapidly metabolise in the liver by CYP3A5 and CYP3A4. Ritonavir a widely used as pharmacokinetic enhancer, that inhibits the CYP3A5 and CYP3A4 isoenzyme in the liver microsomes and therefore it increases the concentration of lopinavir in systemic circulation. Therefore we also used combination tablet formulation of LR-MSNs-NPs for in-vivo assessment and that shows LR-MCM-48 NPs and LR-SBA-15 NPs exhibited better pharmacokinetic properties compared to LR-MCM-41NP, Pure LPV, pure LPV/RTV and LPV/RTV MF. The relative oral bioavailability of LPV in albino wistar rat resulted from LR-MCM-48NPs was about 11.27-fold, 3.35-fold and 1.51-fold higher than that of pure LPV, combination of LPV/RTV and MF of LPV/RTV respectively. Likely from LR-SBA-15NPs relative oral bioavailability of LPV was found 10.95-fold, 3.25-fold and 1.47-folds greater than that of pure LPV, combination of LPV/RTV and MF of LPV/RTV respectively. The reason behind the results is that MCM-48NPs having 3D cubic pores structure which offers easy drug diffusion from the interconnected pores into the dissolution media. From all the above facts revealed that MCM-48NPs contribute faster drug release as compared to MCM-41NPs with 2D hexagonal long channels. Thus,

MCM-48NPs shows more propitious mesoporous carrier giving fast and maximum release compare with MCM-41NPs.

Likely from SBA-15NPs relative oral bioavailability of LPV was found 2.33-fold and 1.43-fold greater than pure LPV and LPV MF. Thus it can be concluded that that using mesoporous silica nanoparticles for LPV which leads to improved dissolution properties and excellent oral bioavailability of LPV.

SBA-15NPs also having 2D hexagonal long channels like MCM-41NPs but have high amount of silanol group present than MCM-41NPs, that adsorb more amount of LPV molecules and also SI-OH groups on SBA-15NPs form very weak bonding with LPV molecules as compared to MCM-41NPs, that can be easily and quickly broken down in dissolution media. Because of all these reasons SBA-15 NPs gave rapid dissolution as well as more diffusion in the dissolution medium.

In vitro Cell Cytotoxicity Studies (MTT Assay) confirmed the biocomatibility synthesised MSNs and explains that composition of MSNs did not contribute to toxicity of Caco2 cells.

Stability studiy results shows the LPV molecules showing good physical and chemical stability with in the mesopores and the mesopores carriers also shows good stability in accelarated stability conditions.

All these results shows mesoporous silica nanoparticles may give a new approach for the development of oral formulations for poorly water-soluble drugs like LPV/RTV.

References

1. https://aidsinfo.nih.gov/drugs/316/kaletra/31/professional (Access on dated 23/4/16)
2. Maria V, Francisco B, Daniel A. Mesoporous materials for drug delivery Angew Chem Int Ed 2007; 46: 7548–7558.
3. Xu W, Riikonen J, Lehto V. Mesoporous systems for poorly soluble drugs. Int J Pharm 2013; 453: 181-197.
4. María V, Francisco B, Montserrat C, Miguel M. Drug confinement and delivery in ceramic implants. Drug Met Let 2007; 1: 37-40.
5. https://www.gograph.com/photo/lopinavir-hiv-drug-molecule-protease-inhibitor-class-gg74939818.html
6. Brunauer S, Emmet P, Teller E. Adsorption of gases in multi molecular layers. J Am Chem Soc 1938; 60: 309–319.
7. Choma J, Jaroniec M, Burakiewicz-Mortka W, Kloske M. Critical appraisal of classical methods for determination of mesopore size distributions of MCM-41 materials. Appl Surf Sci 2002; 196: 216–223.
8. Salonen J, Laitinen L, Kaukonen AM, Tuura J, Björkqvist M, Heikkilä T, Vähä- Heikkilä K, Hirvonen J, Lehto V.P. Mesoporous silicon microparticles for oral drug delivery: loading and release of five model drugs. J Control Rel 2005; 108: 362–374.
9. Heikkilä T, Salonen J, Tuura J, Kumar N, Salmi T, Murzin D.Y, Hamdy M.S, Mul G, Laitinen L, Kaukonen A.M, Hirvonen J, LehtoV. Evaluation of mesoporous TCPSi, MCM-41, SBA-15, and TUD-1 materials as API carriers for oral drug delivery. Drug Deliv 2007; 14: 337–347.
10. Vasconcelos T, Sarmento B, Costa P. Solid dispersions as strategy to improve oral bioavailability of poor water soluble drugs. Drug Discov Today 2007; 12: 1068–1075.
11. Kesisoglou F, Panmai S, Wu Y. Nanosizing. Oral formulation development and biopharmaceutical evaluation. Adv Drug Deliv Rev. 2007; 59: 631–644.
12. Jinno J, Kamada N, Miyake M, et al. Effect of particle size reduction on dissolution and oral absorption of a poorly water-soluble drug, cilostazol, in beagle dogs. J Control Release 2006;111:56–64.

13. O'driscoll C, Griffin B. Biopharmaceutical challenges associated with drugs with low aqueous solubility – the potential impact of lipid-based formulations. Adv Drug Deliver Rev 2008; 60: 617–24.
14. Ambrogi V, Perioli L, Pagano C, Marmottini F, Ricci M, Sagnella A, Rossi C. Use of SBA-15 for furosemide oral delivery enhancement. Eur J Pharm Sci 2012; 46: 43–48
15. Ma Y, Qi L, Ma J, Wu Y, Liu O, Cheng H. Large-pore mesoporous silica spheres: synthesis and application in HPLC. Colloids Surf. A 2003; 229:1–8.
16. Agarwal S, Boddu SHS, Jain R, Samanta S, Pal D, Mitra AK, Peptide prodrugs: Improved oral absorption of lopinavir, a HIV protease inhibitor. International Journal of Pharmaceutics 2008; 359: 7–14.
17. Farmer P, Léandre F, Mukherjee J, Gupta R, Tarter L, Kim JY. Community-based treatment of advanced HIV disease: introducing DOT-HAART (directly observed therapy with highly active antiretroviral therapy). Bull World Health Organ 2001; 79: 1145–1151.
18. Ravi PR, Vats R, Thakur R, Srivani S, Aditya N. Effect of Grapefruit Juice and Ritonavir on Pharmacokinetics of Lopinavir in Wistar Rats. Phytother. Res 2012; 26(10):1490-5
19. Piacenti FJ. 2006. An update and review of antiretroviral therapy. Pharmacotherapy 26: 1111–1133.
20. Pierson T, McArthur J, Siliciano RF. Reservoirs for HIV-1: mechanisms for viral persistence in the presence of antiviral immune responses and antiretroviral therapy. Annu Rev Immunol 2000; 18: 665–708.
21. Serda RE, Gu J, Bhavane RC, Xu, Liu XW, Chiappini C, Decuzzi P, Ferrari M, The association of silicon microparticles with endothelial cells in drug delivery to the vasculature. Biomaterials 2009; 30(9): 2440-2448
22. Santosa HA, Riikonen J, Salonen J Mäkil E, Heikkil T, Laaksonen T, Peltonen L, PekkaLehto V, Hirvonen J. In vitro cytotoxicity of porous silicon microparticles: Effect of the particle concentration, surface chemistry. Acta biomater 2010; 6(7): 2721-2731